

MODELING OF REVERSE OSMOSIS AND PREDICTION  
OF REVERSE OSMOSIS MEMBRANE  
PERFORMANCE

By

KALYAN S. WUNNAVA

Bachelor of Engineering

Osmania University

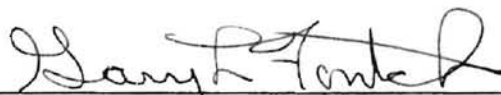
Hyderabad, India

1994

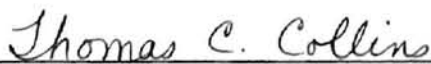
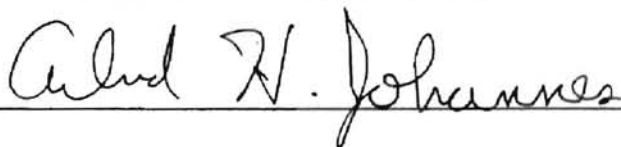
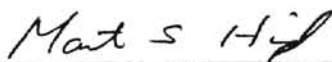
Submitted to the Faculty of the  
Graduate College of the  
Oklahoma State University  
in partial fulfillment of  
the requirements for  
the Degree of  
MASTER OF SCIENCE  
May, 1997

MODELING OF REVERSE OSMOSIS AND PREDICTION  
OF REVERSE OSMOSIS MEMBRANE  
PERFORMANCE

Thesis Approved:



Thesis Advisor



Dean of the Graduate College

## PREFACE

This study deals with modeling of reverse osmosis and prediction of performance of reverse osmosis membranes for four monovalent ions in aqueous solutions. This work is based on work done by Sunil Kar. A computer code is developed to provide the solution to the model and predict the membrane performance.

I am extremely grateful to my advisor, Dr. Gary L. Foutch for his guidance, patience and encouragement. I would also like to express my gratitude to Dr. Martin S. High for his assistance and invaluable suggestions. This work would never have been completed without their inspiration and technical support. I would like to extend my special thanks Dr. Arland H. Johannes and Dr. Martin S. High for their willingness to serve on my thesis defense committee. Thanks are due to Dr. Vikram Chowdiah, Sree Vinay Sunkavalli and Dennis Hussey for their suggestions, and Arunachalam Allagappam for his laboratory assistance. Financial assistance from the School of Chemical Engineering at Oklahoma State University is gratefully appreciated.

Special thanks are due to my parents Krishna Rao and Valli Lakshmi Wunnava, my younger brothers Shiva and Bhanu, to my uncles Dr. Subbarao V. Wunnava, Prasad Wunnava, Dr. Phanindra V. Wunnava and all their family members for their motivation, encouragement and emotional support.

## TABLE OF CONTENTS

Chapter	Page
I. INTRODUCTION.....	1
Principles of Osmosis and Reverse Osmosis.....	1
Modeling of Reverse Osmosis and Prediction of Membrane Performance for High Purity Water Production.....	2
Objective.....	3
Organization.....	3
II. LITERATURE REVIEW.....	4
Membrane Processes.....	4
Fundamentals of Reverse Osmosis.....	7
Reverse Osmosis Membranes.....	7
Recent Advances in RO Membranes.....	8
Osmotic Pressure.....	10
Driving Forces for Transport.....	10
Concentration Polarization.....	11
Performance of RO Membrane.....	13
Recovery.....	13
Rejection.....	13
Factors influencing RO Membrane Performance.....	14
Temperature.....	14
Pressure.....	14
Feed Quality.....	15
Concentration Polarization.....	15
Membrane Element Configuration.....	15
Flow Conditions.....	16
Spiral Wound Modules.....	16
III. MODEL DESCRIPTION.....	18
Introduction.....	18
Model Assumptions.....	19
Explanation of Symbols.....	20
Membrane Transport in Reverse Osmosis.....	21



Transport Equations Applicable to Multicomponent System....	24
Water or Solvent Flux.....	26
Ionic Flux Expressions.....	26
Expression for Average Mass Transfer Coefficient.....	30
Material Balances.....	32
IV. MODEL SOLUTION.....	33
Steps Involved in the Model Solution.....	34
Description of Computer Code.....	35
V. RESULTS AND DISCUSSION.....	37
VI. SEPARATION OF AMINES USING PERVAPORATION.....	61
Introduction.....	61
Pervaporation Experiments for Amine Separation.....	62
Results.....	68
VII. CONCLUSIONS AND RECOMMENDATIONS.....	70
BIBLIOGRAPHY.....	73
APPENDIXES.....	79
APPENDIX A - DERIVATION OF THE CONCENTRATION.....	79
POLARIZATION EFFECT IN REVERSE OSMOSIS	
USING THE FILM CONCEPT	
APPENDIX B - CORRELATIONS USED IN REVERSE OSMOSIS.	82
APPENDIX C -COMPUTER CODE.....	84

## LIST OF TABLES

Table	Page
I. Comparison of Various Membrane Processes.....	6
II. Free Energy and Solute Transport Parameters of Ions.....	38
III. Specifications of Different Cellulose Acetate Membranes.....	39
IV. Comparison of Experimental and Predicted Results.....	40
V. Common Input Data for the Three Feed Compositions of NaCl & KNO <sub>3</sub> .....	41
VI. Prediction of Membrane Performance for Three Different Feed Conditions..	42
VII. The Concentrations of ETA in the Feed, Product and Reject (ppm) at Different Time Intervals for Feed-I.....	65
VIII. The Concentrations of Dimethylamine in the Feed, Product and Reject (ppm) at Different Time Intervals for Feed-II.....	66
IX. The Concentrations of ETA and Sodium in the Feed, Product and Reject (ppm) at Different Time Intervals for Feed-III.....	67

## LIST OF FIGURES

Figure	Page
1. Schematic of a Membrane Process.....	4
2. Effect of Operating Pressure on Product Flux (Flat RO Unit).....	46
3. Effect of Operating Pressure on Product Mole Fractions of Ions (Flat RO Unit)...	47
4. Effect of Operating Pressure on Product Mole Fractions of Ions (Spiral-Wound)	48
5. Variation of pH of the Permeate (Flat-RO Unit).....	50
6. Variation of pH of the Permeate (Spiral-Wound).....	51
7. Effect of Operating Pressure on Product Flux (Spiral-Wound).....	52
8. Effect of Feed Concentration on Product Mole Fractions of Ions (Flat RO Unit)..	53
9. Effect of Feed Concentration on Product Mole Fractions of Ions (Spiral-Wound).	54
10. Effect of Increase in Mass Transfer Coefficient on Ion Separation (Flat RO Unit)	56
11. Effect of Increase in Mass Transfer Coefficient on Product Rate (Flat RO Unit)..	57
12. Effect of Feed Flow Rate on Rejection of Ions (Spiral-Wound).....	58
13. Effect of Feed Flow Rate on Product Flux (Spiral-Wound).....	59
14. Experimental Setup of the Pervaporation Apparatus.....	63

## NOMENCLATURE

$A$	Pure water permeability constant ( $\text{gmole H}_2\text{O}/\text{cm}^2 \cdot \text{atm}$ )
$A_{\text{ch}}$	Area of feed channel of spiral-wound module ( $\text{cm}^2$ )
$A_M$	Area of membrane surface available for transport ( $\text{cm}^2$ )
$B$	Solute permeability constant (atm)
$B_{\text{AV}}$	Average solute permeability constant defined by Equation (3-17) (atm)
$c$	Solution molar density ( $\text{gmole}/\text{cm}^3$ )
$C_{\text{si}}$	Concentration of solute $i$ ( $\text{gmole}/\text{cm}^3$ )
$D$	Diffusivity of solute ( $\text{cm}^2/\text{s}$ )
$D_i$	Diffusivity of ion $i$ ( $\text{cm}^2/\text{s}$ )
$D_{\text{NaCl}}$	Diffusivity of NaCl ( $\text{cm}^2/\text{s}$ )
$D_{\text{SM}}$	Diffusivity of solute in membrane ( $\text{cm}^2/\text{s}$ )
$D_{\text{SW}}$	Diffusivity of solute in water ( $\text{cm}^2/\text{s}$ )
$K$	Partition coefficient or solubility ( $\text{s}/\text{cm}$ )
$k$	Solute mass transfer coefficient ( $\text{cm}^2/\text{s}$ )
$k_{\text{av}}$	Average solute mass transfer coefficient defined by Equation (3-58) ( $\text{cm}/\text{s}$ )
$k_{\text{NaCl}}$	Mass transfer coefficient for NaCl ( $\text{cm}^2/\text{s}$ )
$K_w$	Dissociation constant of water
$J_w$	Volume flux of solvent or water ( $\text{cm}^3/\text{cm}^2 \cdot \text{s}$ )
$N_i$	Molar flux of ion ( $\text{gmole}/\text{cm}^2 \cdot \text{s}$ )
$N_s$	Molar flux of solute ( $\text{gmole}/\text{cm}^2 \cdot \text{s}$ )
$N_w$	Molar flux of water ( $\text{gmole}/\text{cm}^2 \cdot \text{s}$ )
$P$	Operating gauge pressure (atm or psig)
$P_1$	Pressure on feed side of membrane (atm or psig)

$P_3$	Pressure on permeate side of membrane (atm or psig)
$\Delta P$	Pressure difference (atm or psig)
$Q_1$	Feed flow rate ( $\text{cm}^3/\text{min}$ )
$Q_2$	Reject flow rate ( $\text{cm}^3/\text{min}$ )
$Q_3$	Permeate flow rate ( $\text{cm}^3/\text{min}$ )
$R$	Rejection
$T$	Absolute temperature (K)
$V_w$	Partial molar volume of water ( $\text{cm}^3/\text{gmole}$ )
$X$	Mole fraction
$Y$	Recovery (%)
$Z$	Valency
Subscripts	
1	(First subscript) $\text{Na}^+$
2	(First subscript) $\text{Cl}^-$
3	(First subscript) $\text{K}^+$
4	(First subscript) $\text{NO}_3^-$
1	(Second subscript) Feed phase
2	(Second subscript) Concentrated boundary layer phase
3	(Second subscript) Permeate phase
a	$\text{NaCl}$
b	$\text{KNO}_3$
c	$\text{NaNO}_3$
d	$\text{KCl}$
av	Average
ch	Channel
i	Ionic species
M	Membrane
$M_w$	Molecular weight of water
SM	Solute in membrane
SW	Solute in water

NaCl Sodium Chloride

W Water

#### Greek Letters

$\alpha$  Defined by Equation (3-11)

$\beta$  Defined by Equation (3-38)

$\gamma$  Defined by Equation (3-39)

$\eta$  Solution kinematic viscosity (cp)

$\mu$  Solute transport parameter defined by equation (3-33)

$\sigma$  Product of mesh-step and mixing efficiency of a turbulence promoter

$\delta$  Thickness of boundary layer (cm)

$\pi$  Osmotic pressure (atm)

$\Delta$  Difference

#### Abbreviations

CA Cellulose Acetate

CTA Cellulose Tri-Acetate

exp Exponential

RO Reverse Osmosis

TDS Total Dissolved Solids

PVA Polyvinyl Chloride

TFC Thin film composites

## **CHAPTER I**

### **INTRODUCTION**

One of the major developments in the field of chemical engineering in this century is the evolution and substantial growth of membrane technology. Membrane separation processes are playing an increasingly vital role in applications such as water desalination, industrial and municipal waste treatment, and gas separation. Apart from these, membrane processes are receiving wide acceptance in the areas of ultrapure water production, boiler feedwater, drinking water systems, and in pharmaceutical applications. One such process is called reverse osmosis (RO). Since their introduction in the late 1950's and commercialization in the 1960's, RO units have become an integral part in the above mentioned applications.

#### **Principles of Osmosis and Reverse Osmosis**

Osmosis is defined as the spontaneous flow of a pure water into an aqueous solution, or from a less to a more concentrated medium when separated by a semi-permeable membrane. A semi-permeable membrane is one which allows only the water and not other salts or organic molecules to permeate through it. The transport occurs due the chemical potential driving force to equalize the osmotic pressure of the two solutions.

When pressure is applied to the more concentrated side and exceeds the osmotic pressure, the direction of the water flow is reversed, resulting in separation of water from

the solution. Consequently, this process is termed 'Reverse Osmosis,' for convenience, or Hyperfiltration.

### **Modeling Reverse Osmosis and Prediction of Membrane Performance for High Purity Water Production**

The knowledge about the individual ionic rejection or permeation rates is very important for any high-purity water production system using RO since it provides information about the required feed flow rate and the effective life of membrane before fouling. With RO, 90% to 95% removal of total dissolved solids (TDS) can be achieved, while removal of ions takes place to a varying degree dependent primarily on their sizes.

Much of the earlier research was focused on understanding the transport in RO membranes (Sourirajan 1970; Kedem and Katchalsky 1958; Lonsdale et al., 1965). A variety of models exist to describe the transport through RO membranes. Most of these mass transport models deal with the systems of aqueous solution with one solute only. Practical applications of RO generally deal with multicomponent systems. In the high purity water industry, product water quality is usually specified in terms of concentration of ions. Moreover, the tolerance limits for the concentration of ions present varies with the industry. Therefore, the conventional practice of using the total dissolved solids (TDS) for product water quality is inadequate. Hence, multicomponent RO models and appropriate membrane performance prediction methods are of great interest. However, only very few studies have been reported in these areas. Rangarajan et al. (1976, 1978a, 1978b, 1979, 1984 and 1985) and Matsuura et al. (1975 and 1985) have done extensive work in the area of mixed solute systems. Extension of the existing models to



multicomponent systems offers lot of complexities like non-availability of osmotic pressure data, unknown ionic-interactions, parameter determination and extensive experimental verification.

### **Objective**

Over the decades, RO has achieved great technological advancement in terms of its design and applications. However, multicomponent system modeling and performance prediction have not been treated as thoroughly as the single solute systems. The objective of this thesis is to focus on multicomponent system consisting of  $\text{Na}^+$ ,  $\text{Cl}^-$ ,  $\text{K}^+$  and  $\text{NO}_3^-$  ions in the aqueous solution, and predict the performance of cellulose acetate reverse osmosis membranes for these ions. Although the model can be used for any four ions and for any reverse osmosis membrane. An attempt is also made to investigate the effect of spiral-wound geometry of the module by using a suitable mass transfer coefficient correlation with the appropriate assumptions.

Also, a small part of the objective is to present some results obtained from a set of preliminary experiments with amine separation using pervaporation.

### **Organization**

This thesis is divided into seven chapters. Some theoretical background about reverse osmosis can be found in Chapter II. The multicomponent model description is given in Chapter III. The solution to the model is discussed in Chapter IV. The results of performance prediction are presented in Chapter V. Some experimental work with the separation of amines is briefly outlined in Chapter VI. Finally, in Chapter VII, conclusions are drawn based on the work done in this thesis, and recommendations for the further effort in this direction are highlighted.

## CHAPTER II

### LITERATURE REVIEW

A brief discussion of membrane processes with particular emphasis on reverse osmosis relevant to the work done in this thesis is presented here. A comprehensive literature review on historical development and mechanisms of reverse osmosis, various transport models, design methods, high-purity water applications, and comparison between reverse osmosis and ion-exchange processes can be found in Kar (1994).

#### Membrane Processes

A membrane is the most important part of every membrane process. A membrane functions like a permselective barrier allowing certain species to pass through while preventing the passage of dissolved and suspended particle. A schematic of a typical membrane process is shown in Figure 1.

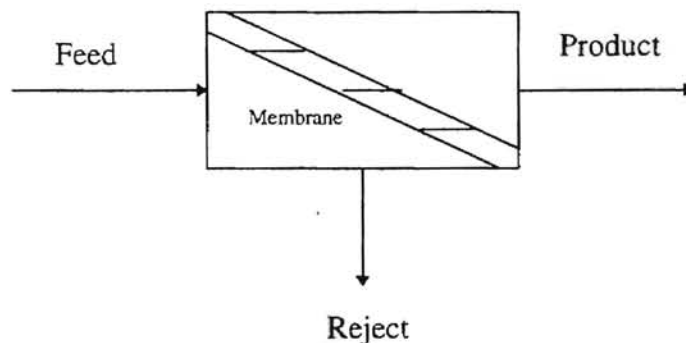


Figure 1: Schematic of a Membrane Process

The various types of commercial membrane processes are:

1. Microfiltration
2. Ultrafiltration
3. Nanofiltration
4. Reverse Osmosis
5. Electrodialysis
6. Gas Separation
7. Pervaporation

Microfiltration, ultrafiltration, nanofiltration and reverse osmosis are comparable processes with a hydrostatic pressure difference as a driving force. They differ principally in the size of the particles separated by the membrane.

Electrodialysis is a membrane process to remove ions from aqueous solutions. Here the driving force is an electrical potential difference which causes mass transport of ionic species through an ion-exchange membrane.

In gas separation, a mixed gas feed at an elevated pressure is passed across the surface of the membrane that is selectively permeable to one of the components of the feed. The process produces a permeate enriched in more permeable species and a residue enriched in the less permeable species.

Pervaporation is a relatively new process that has elements in common with reverse osmosis and gas separation. It differs from other membrane processes in that the membrane constitutes a barrier between the feed in the liquid phase and permeate in the

gas phase, and separation takes place under the influence of a concentrated gradient.

Comparison of various types of membrane separation processes is given in the Table I (Cartwright, 1995).

Table I: Comparison of various membrane processes.

Membrane Process	Driving Force	Membrane Material	Operating Pressure(psig)
Microfiltration	Pressure	Nylon, Teflon & Cellulosics	<10
Ultrafiltration	Pressure	Polymers from Polysulphone etc.	10-100
Nanofiltration	Pressure	CA, CTA etc.	50-200
Reverse Osmosis	Pressure	CA, CTA & TFC	250-1500
Electrodialysis	Electric Potential	Ion-exchange membranes	-
Gas Separation	Partial Pressure	Solution-diffusion membranes	-
Pervaporation	Concentration gradient	PVA composites silicones & CA	-

Membranes processes possess certain advantages which make them unique when compared to other liquid/solid separation operations. These include (Cartwright, 1995):

1. Continuous processes, resulting in automatic and uninterrupted operation
2. Low energy consumption involving neither temperature nor phase changes in general
3. Modular design; no significant size limitations
4. Low maintenance cost requirements

5. No effect on form or chemistry of contaminants

6. No chemical addition requirements

### **Fundamentals of Reverse Osmosis**

Reverse Osmosis is the first membrane based separation process to be widely commercialized. The literature on the subject of reverse osmosis is extensive. Here an attempt is made to present a brief review of topics related to reverse osmosis bearing some direct relevance to the work done in this thesis.

#### Reverse Osmosis Membranes

A review of RO membranes can be found in Sourirajan (1977), Belfort (1984), Allegrezza (1988), and Ikeda and Tomaschke (1994). Loeb and Sourirajan developed the first asymmetric cellulose diacetate membranes. A major research and development effort, using their work as a basis, took place through the 1960's and 1970's, with substantial sponsorship by Department of the Interior, Office of Saline Water.

A typical RO membrane is composed of a dense surface skin and a porous substructure. Salt rejection occurs at surface skin layer, with the permeate passing into the porous sublayer. Two basic types of membranes in commercial use are: Asymmetric and thin film composite (TFC). Asymmetric membranes are formed using the same polymer for the dense surface skin and the porous sublayer. Cellulose acetate, cellulose triacetate, and polyamide are common polymers used in the preparation on asymmetric membrane. In thin film composite membranes, the surface skin and microporous sublayer are formed from two different polymers. Commonly, aromatic polyamide is used for the surface skin and a graded polysulfone resin is used in the sublayer.

Each membrane type offers certain advantages and disadvantages. Cellulose acetate membranes are lower in cost, and are chlorine resistant. However, the membranes tend to chemically degrade outside a pH range of 5 to 8. These membranes are also susceptible to biological degradation and therefore require chlorine addition to the feedwater to control bacterial growth. Aromatic polyamide membranes offer hydrolytic stability and better salt and organic rejection, and better resistance to biological degradation. But they are higher in cost than cellulose acetate (CA) membranes and have zero tolerance for free chlorine in the feedwater (Harfst, 1995).

#### Recent Advances in RO Membranes

Historically, cellulose acetate has been the most important polymer in the development membranes suitable for the RO applications. More recently, many kind of ultra thin film composite RO membranes have been developed by interfacial polymerization, or in situ polymerization. Cadotte et al. (1980) originally demonstrated the utility of interfacial polycondensation of trimesoyl chloride and m-phenylene diamine in preparing composite membranes with good properties. Sundet et al. (1987) extended the original aromatic-aromatic polyamide chemistry of Cadotte and Peterson (1990) to aromatic-cyclo-aliphatic structures including the product of interfacial polyamidation. New composite RO membranes based on m-phenylene diamine and 1,2,3,4-cyclopentane tetra carboxylic acid polyamide have been developed. These membranes exhibit the monovalent ion rejection of more than 99% and high flux (Ikeda and Tomaschke, 1994).

Extensive work has been done by Cadotte (1981) in the preparation of polyvinyl alcohol based composite membranes. Polyvinyl alcohol by virtue of its hydrophilic

nature is a useful building block in RO membranes, and is also commonly used as a protective surface coating on the top of composite membranes. Here its purpose is to enable one to handle and fabricate the membrane into spiral-wound elements without causing damage to the ultrathin barrier layer.

Two composite membranes with significant chlorine resistance, NTR-729HF and NTR-739HF, have been commercialized by Nitto Denko (a membrane manufacturer) for use in desalinating low salinity brackish waters. These membranes have particularly found use in the preparation of ultrapure water for the semiconductor industry. The performance of NTR-729HF and NTR-739HF is comparable to CA membranes for inorganic solutes, while they exhibit better rejection characteristics than CA for the organic compounds like ethanol and isopropanol.

In addition to thin film composites and asymmetric RO membranes, other types of RO membranes have been developed. But it is not economically viable for their wide commercial use. Some of these membranes are:

1. Composite membrane formed by plasma polymerization.
2. Dynamic RO membranes
3. Hollow fiber glass RO membranes

Much of the future research is likely to be focused on the development of chlorine resistant membranes and higher flux/low pressure membranes for the treatment of brackish waters. Membranes with better resistance to fouling, especially bio-fouling, are also the subject of growing interest.

## Osmotic Pressure

The pressure that must be applied to prevent the flow of a dilute solution into a concentrated solution when separated by semi-permeable membrane is called osmotic pressure. Osmotic pressure is a colligative property of a solution. The osmotic pressure of a solution  $\pi_i$ , is related to mole fraction of the solvent,  $X_{wi}$ , as (Castellan, 1971):

$$\pi_i = -\left(\frac{RT}{V_w}\right) \ln X_{wi} \quad (2-1)$$

where  $R$  is the universal gas constant,  $T$  is the temperature and  $V_w$  is the partial molar volume of the solvent. For dilute solutions, the above equation simplifies to the Van't Hoff equation (Castellan, 1971).

$$\pi_i = C_{si} RT \quad (2-2)$$

where  $C_{si}$  is the concentration of solute.

## Driving Forces for Transport

In reverse osmosis systems, the driving force of interest are pressure and concentration which lead to flux of solvent and solute respectively. The solvent flux is directly proportional to the effective pressure driving force described by:

$$N_w = J_w c = A(P - \Delta\pi) \quad (2-3)$$

where  $N_w$  is the molar flux of solvent,  $J_w$  is the volume flux of the solvent,  $c$  is the molar density of the solution and  $A$  is the solvent permeability constant,  $P$  is the gauge pressure on higher pressure side of the membrane, and  $\Delta\pi$  is the osmotic pressure difference between solvent on the high and low pressure side of the membrane. The effective driving pressure,  $\Delta P$ , for the solvent flux through the membrane given by:



$$\Delta P = P - \Delta \pi \quad (2-4)$$

is the pressure required to overcome the osmotic pressure of the solution to liberate the pure water and to overcome the membrane resistance to the flow.

### Concentration Polarization

In reverse osmosis, when solute is rejected by the membrane, the solute concentration near the membrane surface increases. Until the steady state condition is reached, convective flux of ions or solutes to the membrane is greater than back diffusion to the bulk solution. This results in buildup in concentration of the rejected species, and is referred to as Concentration Polarization.

The effect of concentration polarization can be modeled by two different approaches. The first approach is by the numerical integration of the transport equations, which is complex and can be found in Rautenbach and Albrecht (1989). The second approach is based upon film theory (Bird et al., 1960), which is considered here. This approach was originally proposed by Sourirajan (1970), based on the concept of mass transfer coefficients. According to film theory, even in the turbulent flow conditions, there exists a laminar boundary layer in the vicinity to the membrane surface. During the transport process, steady state is reached when the convective transport of the solute to the membrane surface is counter balanced by a diffusive flow of the rejected solutes from the membrane surface. The convective flux of the solute to the membrane is given by:

$$\frac{C_s}{c} (N_s + N_w) \quad (2-5)$$

where  $C_s$  and  $c$  are concentration of solute and molar density of the solution,  $N_s$  and  $N_w$  are flux of solute and solvent, respectively. The back diffusion of the solute from membrane can be assumed to follow Fick's law,

$$D_{sw} \frac{dC_s}{dy} \quad (2-6)$$

where  $D_{sw}$  is the diffusivity of the solute and is the rate of change of solute concentration. At steady state, flux through the membrane can be represented as:

$$N_s = \frac{C_s}{c}(N_s + N_w) - D_{sw} \frac{dC_s}{dy} \quad (2-7)$$

Let  $C_{s1}$ ,  $C_{s2}$ , and  $C_{s3}$  be the concentration of solute in the bulk solution, at membrane surface, and in the permeate respectively, and ' $\delta$ ' the thickness of boundary layer.

Rearrangement of Equation (2-7) with appropriate boundary conditions (Sourirajan, 1970), gives:

$$C_{s2} = C_{s3} + (C_{s1} - C_{s3}) \exp\left(\frac{N_s + N_w}{c} \frac{\delta}{D_{sw}}\right) \quad (2-8)$$

Defining the mass transfer coefficient in the conventional manner of the film theory (Bird et al., 1960),

$$k = \frac{D_{sw}}{\delta} \quad (2-9)$$

Substituting the above relation in the Equation (2-8), we have:

$$C_{S2} = C_{S3} + (C_{S1} - C_{S3}) \exp\left(\frac{N_s + N_w}{kc}\right) \quad (2-10)$$

Equation (2-10) expresses the concentration of the solute in the boundary layer and represents the concentration polarization phenomenon. A more detailed derivation of this phenomenon can be found in Appendix A.

### **Performance of RO Membrane**

The performance of RO membranes is represented commonly by two expressions. They are:

#### Recovery:

Recovery is defined as the percentage of the feed flow that is converted to product or permeate. Typically, it is about 70% to 80% in practical situations. Recovery is inversely proportional to the concentration of the feed water. Mathematically,

$$Y = \frac{Q_3}{Q_1} \times 100 \quad (2-11)$$

Where Y is the recovery,  $Q_3$  is the permeate flow, and  $Q_1$  is the feed flow rate.

#### Rejection:

Different membranes exhibit different rejection characteristics for ions and soluble organics. Higher rejection rates are always accomplished by lower recovery rates. Not all ions are equally rejected. For dilute feed, monovalent ions are rejected to about 97%, whereas the divalents are generally rejected to about 99% or higher. RO units reject organics well if the molecular weight of organics is greater than 200 for the cellulosic

membranes and 100 for thin film composite membranes. Rejection is expressed as the percentage and is defined in terms of molal concentrations of feed and permeate,  $C_{S1}$  and  $C_{S3}$ , respectively.

$$R = \left( \frac{C_{S1} - C_{S3}}{C_{S1}} \right) \times 100 \quad (2-12)$$

where R is the rejection.

#### Factors influencing RO Membrane Performance:

In general, the following factors affect the performance and efficiency of RO separation systems.

##### Temperature:

The effect of temperature on rejection is approximately linear. As the feed temperature increases, viscosity of the feed decreases, thereby facilitating the transport through the membrane, and resulting in an increase of solute and solvent fluxes. Since most membrane polymers are thermoplastic, they become softer and more compressible as the temperature increases. The combination of temperature and pressure can cause irreversible compaction in some polymers (e.g., cellulosic) resulting in premature failure. For all practical purposes, flux through the membrane increases by 3% for every 1°C rise in the temperature.

##### Pressure:

The permeate flow rate is directly proportional to the net driving pressure. The net driving pressure is defined as the total applied gauge pressure minus the sum of osmotic pressures of the feed and the permeate. Osmotic pressure increases as the

concentration of the solute increases. In most water purification applications, the total dissolved solids is sufficiently low ( $\text{TDS} < 10000 \text{ ppm}$ ) so that osmotic pressure is not significant. Net driving pressures range from as low as 30 psig for microfiltration systems to approximately 1500 psig, considered to be the practical limit for available reverse osmosis systems.

#### Feed Quality:

The chemical composition of feed stream greatly affects the performance of the membrane. Presence of certain chemicals results in degradation of membrane polymer. Cellulosic membrane polymers are subject to hydrolysis by high pH and are best operated in the pH range of 5-7. Polyamide and most TFC polymers are degraded by strong agents such as chlorine, and operated at a wider pH range of 5-9. Suspended solids also represent a potential problem. The lower their concentration, the better is the membrane performance.

#### Concentration Polarization:

This phenomenon is associated with reverse osmosis. The fouling layer like dirt, scale, biofilm, etc. builds up on the membrane surface and prevents normal mixing of rejected ionic salts throughout the flowing stream. This buildup of salts can produce additional scaling and further fouling. This produces permeate of lower quality with higher TDS.

#### Membrane Element Configuration:

The configuration of membrane polymer in an element design has a direct bearing on the resistance to the membrane to fouling. The four main types of membrane

element configurations are tubular, fine hollow fiber, spiral-wound, and plate and frame. Packing of maximum possible area into an element without making it too large or heavy is highly desirable. The element designs that provide the greatest packing density also have the lowest resistance to fouling. The most widely used configuration is spiral-wound, as its packing density is medium-low compared to other configurations, and its tolerance towards the suspended solids is fairly high.

#### Flow Conditions:

Membrane elements are much less susceptible to fouling from suspended or precipitated solids if the flow through the elements is turbulent. Normally, they are operated at Reynolds numbers of 4000 or above, which represents turbulent flow conditions for the membrane systems.

### **Spiral Wound Modules**

Membrane materials for all practical applications need to be packed in a device known as membrane element or module. The particular way that the membrane polymer is configured in an element design has a direct bearing on the resistance of the membrane to fouling. As mentioned earlier, of the four different membrane configurations, spiral-wound is the most popular. .

The following are the requirements for a membrane module (Kar, 1994).

1. Mechanical stability, such as supporting a fragile membrane under high operating pressures
2. Hydrodynamic consideration, such as minimizing concentration polarization, and improving the membrane performance

3. Economic considerations, such as high membrane packing density, low capital and maintenance costs, ease in replacement of membranes, etc.

Detailed description of spiral-wound modules can be found in Ko and Guy (1988), Allegrezza (1988), and Kreman and Riedinger (1971). These modules consist of flat sheet membranes 40 to 60 inches wide with fabric spacers in between these membranes, and are spirally wound around a central core or pipe. The three sides of these membranes are closed. The fourth, open side is sealed around the openings of a central core. The sandwiched spacers direct the water that permeates from the outside, to flow into the openings of the central pipe. The spacers are mesh-like construction designed to create turbulence in the flowing feedwater stream. The feedwater enters from one end of a tube that surrounding the core, and the reject leaves from the other. The permeate water emerges through the central pipe.

## **CHAPTER III**

### **MODEL DESCRIPTION**

#### **Introduction**

As mentioned in Chapter I, the development of multicomponent models and suitable methods for predicting membrane performance are an areas of fundamental importance in reverse osmosis transport, and is considerably more complex than it is for single solute systems. Experiments are needed to determine different transport properties such as diffusivity, mass transfer coefficient, osmotic pressure, etc. The data on osmotic pressure for different ions are not extensive in the literature. For multicomponent system involving several ions, determining the osmotic pressure even by experimentation is extremely difficult.

Some of the earliest investigation with multicomponent systems was done by Sourirajan (1963 and 1964). Hodgson (1970) first reported the development of a suitable method for predicting membrane performance for multicomponent system involving several ions in aqueous solution. But the effect of concentration polarization was neglected in their analyses. This limits the significance of their work since concentration polarization plays an important role in RO. Rangarajan et al. (1978a, 1978b, 1979 and 1985) have reported some detailed analysis of multicomponent systems applicable to cellulose acetate membranes, and have presented some experimental data. The basis for multicomponent system modeling is a membrane mass transport model. An excellent



review of the most common transport models can be found in Kar (1994). Most of these models are proposed for single salt systems, which can be extended to describe more complex multicomponent systems.

The objective of this thesis is to predict the performance (ion separation and product rate) of a reverse osmosis membrane. Here cellulose acetate membranes of different surface porosities for different aqueous feed solutions containing the monovalent ions  $\text{Na}^+$ ,  $\text{K}^+$ ,  $\text{Cl}^-$  and  $\text{NO}_3^-$  are chosen for the study. The model is based on the theoretical framework proposed by Kar (1994) for rejection of ions in multicomponent systems using Kimura-Sourirajan analysis. His work is based primarily on work by Rangarajan et al. (1978a, 1978b, 1979 and 1985), and takes into account the effect of geometry of spiral-wound module. Here, an attempt is made to take a step ahead of single solute systems, and predict the performance of RO cellulose acetate membrane for the above chosen four ions.

### **Model Assumptions**

The model is based on the following assumptions:

1. There is no ion-ion or ion-membrane interaction in the multicomponent feed water system.
2. The feed water is relatively dilute and free of particulates.
3. The molar density of the solution is constant throughout the system. i.e.,  
$$c_1 = c_2 = c_3 = c$$
4. The flux of solvent water is high in comparison to that of all ions through the membrane. i.e.,

$$N_w \gg \sum N_i$$

5. The osmotic pressure is solution is proportional to the sum of the mole fraction of all the ions, i.e.,

$$\pi(\sum X_i) = B_{AV} \sum(X_i)$$

where,  $B_{AV}$  is a average proportionality constant representing the slope of mole fraction versus osmotic pressure plots of the single salts.

6. The membrane is uniform with negligible charge density.
7. Fluid properties are essentially constant. Temperature dependence of osmotic pressure and diffusivities of ions is assumed to be negligible.
8. Module is spiral-wound type. The curvature of the channel can be neglected since the ratio of channel height to the module diameter is very small.
9. Concentration polarization is absent on the low pressure side of the membrane and that on the high pressure side of the membrane is evaluated by the film theory.
10. For any salt or ion, the ratio of diffusivity through the membrane to that of in water is a constant (Hoffer and Kedem, 1972). i.e.,

$$\frac{D_{SM}}{D_{SW}} = \frac{D_{iM}}{D_i} = \text{constant}$$

### **Explanation of Symbols**

A short description of the symbols used in this model is given here. All symbols are defined at the beginning of the thesis. In an RO unit, three general phases involved are solute or ion phase, the solvent or water phase, and the membrane phase. The subscripts S, W, and M refer to salt, water and membrane phase, respectively. Symbol X

is used to denote the mole fraction of the ions or salts. In this work, four ions are considered. The cations ( $\text{Na}^+$  and  $\text{K}^+$ ) are represented by the first subscript 1 and 2, and the anions ( $\text{Cl}^-$  and  $\text{NO}_3^-$ ) are represented by first subscript 3 and 4, respectively. The second subscript M, 1, 2, or 3 refers to the indicated phase (M=membrane phase, 1=bulk feed solution phase, 2=concentrated boundary layer phase on the high pressure side of the membrane, and 3=permeate phase on the atmospheric side of the membrane). The ions are collectively represented by the symbol 'i'. Numerical subscripts a, b, c and d refer to single salts NaCl,  $\text{KNO}_3$ ,  $\text{NaNO}_3$  and KCl, respectively. The solute transport parameter, according to the Kimura-Sourirajan model is denoted by  $\left(\frac{D_{sw}K}{\delta}\right)$ . Other symbols are presented in the nomenclature section of this thesis.

### **Membrane Transport in Reverse Osmosis**

The membrane transport in reverse osmosis for single solute system is explained by various transport models. Depending on the transport mechanism, expressions for the solute or ion and solvent flux completely describe the reverse osmosis separation process. According to Kimura-Sourirajan model, the basis for work done by Kar (1994), reverse osmosis separation is governed by surface phenomenon. The RO membrane is porous and heterogeneous at all levels of solute separation, and with respect to systems involving aqueous electrolytic solutions and cellulose acetate membranes. The ions are repelled in the vicinity of the membrane surface, and water is preferentially sorbed at the membrane solution interface. The solute flux  $N_s$ , is proportional to the concentration gradient across the membrane and is expressed as:

$$N_s = D_{SM} \left( \frac{c_{M2} X_{SM2} - c_{M3} X_{SM3}}{\delta} \right) \quad (3-1)$$

where  $D_{SM}$  is the diffusivity of the solute through the membrane,  $X_{SM2}$  and  $X_{SM3}$  are mole fraction of solute in the membrane in equilibrium with  $X_{S2}$  and  $X_{S3}$ , respectively. The molar densities,  $c_{M2}$  and  $c_{M3}$  correspond to  $X_{SM2}$  and  $X_{SM3}$  in the membrane. Assuming a linear relationship between  $X_S$  and  $X_{SM}$ ,

$$KcX_S = c_M X_{SM} \quad (3-2)$$

where  $K$  is the partition coefficient. Using the above relationship, solute flux can be expressed as:

$$N_s = \left( \frac{D_{SM} K}{\delta} \right) (c_2 X_{S2} - c_3 X_{S3}) \quad (3-3)$$

where the quantity  $\left( \frac{D_{SM} K}{\delta} \right)$  is called the solute transport parameter.

The solvent flux,  $N_w$ , through the membrane is proportional to the effective pressure gradient.

$$N_w \propto \Delta P \quad (3-4)$$

The effective pressure gradient can be expressed as:

$$\Delta P = (P_1 - P_3) - \Delta \pi \quad (3-5)$$

where  $P_1$  and  $P_3$  are the pressure at the feed and at the permeate, respectively. Since the permeate is at atmospheric pressure,  $(P_1 - P_3)$  can be written as operating gauge pressure,  $P$ .

The osmotic pressure gradient through the membrane,  $\Delta \pi$ , can be expressed as

$$\Delta \pi = \pi(X_{S2}) - \pi(X_{S3}) \quad (3-6)$$

where  $\pi(X_{S2})$  and  $\pi(X_{S3})$  are the osmotic pressure of the feed at membrane and at the permeate, respectively. So Equation (3-4) can be written as:

$$\Delta P = [P - \{\pi(X_{S2}) - \pi(X_{S3})\}] \quad (3-7)$$

Substituting in Equation (3-4), the solvent flux is given by:

$$N_w = A [P - \{\pi(X_{S2}) - \pi(X_{S3})\}] \quad (3-8)$$

where A is the pure water permeability constant. As can be seen, the concentration of the solute at the membrane,  $X_{S2}$ , is needed to compute the solute and solvent fluxes through the membrane. This can be obtained from the phenomenon of concentration polarization explained in Chapter II. According to this phenomenon, based upon film theory,

$$\frac{N_s + N_w}{kc_1} = \ln \left[ \frac{X_{S2} - X_{S3}}{X_{S1} - X_{S3}} \right] \quad (3-9)$$

For the detailed derivation, refer to Kar (1994). Since the solute flux is assumed to be negligible in comparison to solvent flux,  $(N_s + N_w)$ , is effectively replaced by  $N_w$ .

Therefore, Equation (3-8) can be rearranged in terms of  $X_{S2}$  as:

$$X_{S2} = X_{S3} + (X_{S1} - X_{S3})\alpha \quad (3-10)$$

where,

$$\alpha = \exp \left( \frac{N_w}{kc_1} \right) \quad (3-11)$$

The solute mole fraction of the permeate can be expressed as

$$X_{S3} = \left( \frac{N_s}{N_s + N_w} \right) \quad (3-12)$$

Equations (3-3), (3-8), (3-10) and (3-12) completely describe the RO transport of a single solute the membrane.

### **Transport Equations Applicable To Multicomponent System (for example, Na<sup>+</sup>, K<sup>+</sup>, Cl<sup>-</sup> and NO<sub>3</sub><sup>-</sup>)**

The basic transport equations developed for reverse osmosis using the Kimura-Sourirajan model for single solute systems can be extended to multicomponent systems (Rangarajan et al., 1978a, 1978b, 1979 and 1984). The equations analogous to single solute systems can be derived for mixed solute systems by a common approach. Only appropriate modifications in the transport equations are necessary.

#### Water or Solvent Flux Expression:

Using the Equation (3-8), the solvent or water flux expression for a multicomponent system can be written as:

$$N_w = A[P - \{\pi(X_{i2}) - \pi(X_{i3})\}] \quad (3-13)$$

According to Assumption-5, using the appropriate expression for osmotic pressure, the above equation can be expressed as:

$$N_w = A[P - B_{AV} \{(\sum X_{i2}) - (\sum X_{i3})\}] \quad (3-14)$$

The expression equivalent to Equation (3-10) for mixed solute system is given by:

$$X_{i2} = X_{i3} + (X_{i1} - X_{i3})\alpha \quad (3-15)$$

Replacing the mole fractions of ions in the concentrated boundary layer,  $X_{i2}$ , in the above solvent flux expression, in terms of mole fractions of ions in the feed and in the permeate using Equation (3-14), we have,

$$N_w = A[P - B_{AV}\{(\sum X_{i2}) - (\sum X_{i3})\}]\alpha \quad (3-16)$$

where  $B_{AV}$  is the proportionality constant obtained from mole fraction versus osmotic pressure plots for single solutes a, b, c and d, and is expressed as:

$$B_{AV} = \frac{B_a + B_b + B_c + B_d}{8} \quad (3-17)$$

since there are eight ions involved (Rangarajan et al., 1978a).

The general electroneutrality condition or the charge balance equation for the feed and permeate phases is given by:

$$\sum Z_i X_{i1} = 0 \quad (3-18)$$

$$\sum Z_i X_{i3} = 0 \quad (3-19)$$

respectively, where  $X_{i1}$  and  $X_{i3}$  include  $H^+$  and  $OH^-$  ions. The similar condition for the ionic flux can be written as:

$$\sum Z_i N_i = 0 \quad (3-20)$$

where  $Z_i$  is the valency of the ion 'i'.

Applying the above charge balance equation for the system under consideration, we get,

$$Na^+ + K^+ + H^+ = Cl^- + NO_3^- + OH^- \quad (3-21)$$

Substituting Equations (3-18) and (3-19) in the Equation (3-16),

$$N_w = AP - 2AB_{AV}(\sum Z_i X_{i1} - \sum Z_i X_{i3})\alpha \quad (3-22)$$

which represents the final equation for the solvent flux for the mixed solute system. The minimum applied pressure needed to produce flux can be obtained from the Equation (3-22). At a pressure below the minimum required pressure, the product flux and the product mole fractions of the ions is equal to zero. i.e.,

$$N_w = 0$$

$$X_{i3} = 0$$

$$\alpha = 0$$

Therefore, from the Equation (3-22), the minimum pressure is given by:

$$P_{\min} = 2B_{AV}\Sigma Z_i X_{i1} \quad (3-23)$$

and is dependent on the mole fractions of the ions in the feed or the concentration of the feed.

#### Ionic Flux Expressions:

The general ionic flux expression can be written as (Kar, 1994):

$$N_i = \left( \frac{D_{iM} K_{i2}}{\delta} \right) cX_{i2} - \left( \frac{D_{iM} K_{i3}}{\delta} \right) cX_{i3} \quad (3-24)$$

where  $i = 1, 2, 3$  and  $\delta$ , the thickness of boundary layer near the membrane surface.

For ions 1, 2, and 3, Equation (3-24) can be written as

$$N_1 = \left( \frac{D_{1M} K_{12}}{\delta} \right) cX_{12} - \left( \frac{D_{1M} K_{13}}{\delta} \right) cX_{13} \quad (3-25)$$

$$N_2 = \left( \frac{D_{2M} K_{22}}{\delta} \right) cX_{22} - \left( \frac{D_{2M} K_{23}}{\delta} \right) cX_{23} \quad (3-26)$$

$$N_3 = \left( \frac{D_{3M} K_{32}}{\delta} \right) cX_{32} - \left( \frac{D_{3M} K_{33}}{\delta} \right) cX_{33} \quad (3-27)$$

and

$$N_4 = \left( \frac{D_{4M} K_{42}}{\delta} \right) cX_{42} - \left( \frac{D_{4M} K_{43}}{\delta} \right) cX_{43} \quad (3-28)$$

respectively.



The mole fractions of ionic species 1, 2, 3, and 4 in the concentrated boundary layer is given by:

$$X_{12} = X_{13} + (X_{11} - X_{13})\alpha \quad (3-29)$$

$$X_{22} = X_{23} + (X_{21} - X_{23})\alpha \quad (3-30)$$

$$X_{32} = X_{33} + (X_{31} - X_{33})\alpha \quad (3-31)$$

$$X_{42} = X_{43} + (X_{41} - X_{43})\alpha \quad (3-32)$$

The ionic transport parameter  $\left(\frac{D_{iM}K_i}{\delta}\right)$ , in the Equation (3-24) is expressed in terms of solute transport parameter  $\left(\frac{D_{AM}K}{\delta}\right)$ , for the different single salts, solution phase ionic concentrations  $cX_i$ , and diffusivities of ions  $D_i$ , and those of salts a, c and d ( $D_a, D_c$  and  $D_d$ ) corresponding to diffusivities of NaCl, NaNO<sub>3</sub>, and KCl in water. For the detailed derivation, refer to Rangarajan et al. (1978b).

Let solute parameter be represented by ' $\mu$ '. i.e.,

$$\mu = \left(\frac{D_{AM}K}{\delta}\right) \quad (3-33)$$

The ionic transport parameter applicable to the solution phases 2 and 3 can be written as:

$$\left(\frac{D_{1M}K_1}{\delta}\right) = \left[\frac{cX_3 + \beta cX_4}{cX_1 + \gamma cX_2}\right]^{\frac{1}{2}} \left(\frac{D_1\mu_a}{D_a}\right) \quad (3-34)$$

$$\left(\frac{D_{2M}K_2}{\delta}\right) = \left[\frac{cX_3 + \beta cX_4}{cX_2 + \gamma^{-1}cX_1}\right]^{\frac{1}{2}} \left(\frac{D_2\mu_d}{D_d}\right) \quad (3-35)$$

$$\left(\frac{D_{3M}K_3}{\delta}\right) = \left[\frac{cX_1 + \gamma cX_2}{cX_1 + \beta cX_4}\right]^{\frac{1}{2}} \left(\frac{D_3\mu_a}{D_a}\right) \quad (3-36)$$

$$\left(\frac{D_{4M}K_4}{\delta}\right) = \left[\frac{cX_1 + \gamma cX_2}{cX_4 + \beta^{-1}cX_3}\right]^{\frac{1}{2}} \left(\frac{D_4\mu_c}{D_c}\right) \quad (3-37)$$

where,

$$\beta = \left(\frac{K_a}{K_c}\right)^2 = \frac{(D_a/D_c)^2 \mu_c^2}{\mu_a^2} \quad (3-38)$$

and

$$\gamma = \left(\frac{K_a}{K_d}\right)^2 = \frac{(D_a/D_d)^2 \mu_d^2}{\mu_a^2} \quad (3-39)$$

According to Assumption-4,

$$N_w \gg \sum N_{i3} \quad (3-40)$$

Therefore, ionic mole fractions in the permeate are given by:

$$X_{i3} = \frac{N_{i3}}{N_w + \sum N_{i3}} \approx \frac{N_{i3}}{N_w} \quad (3-41)$$

Hence, the ionic fluxes can be expressed in terms of mole fractions in the permeate as:

$$N_{i3} = X_{i3}N_w \quad (3-42)$$

Upon substitution of Equations (3-29), (3-30), (3-31) and (3-32) into ionic flux equations given by (3-25), (3-26), (3-27) and (3-28) respectively, and further substitution of Equations (3-34), (3-35), (3-36) and (3-37) into the same ionic flux equations, followed by rearrangement, simplification and final usage of Equation (3-41), we obtain expressions for mole fraction of ions  $\text{Na}^+$ ,  $\text{K}^+$ ,  $\text{Cl}^-$  and  $\text{NO}_3^-$  in the permeate.

The mole fraction for  $\text{Na}^+$  is given by:

$$X_{13} = \Psi_1 \left[ \left\{ X_{13} + (X_{11} - X_{13})\alpha \right\} (\Omega_1)^{1/2} - X_{13} \left\{ \frac{X_{33} + \beta X_{43}}{X_{13} + \gamma X_{23}} \right\}^{1/2} \right] \quad (3-43)$$

where,

$$\Psi_1 = \frac{\mu_a c}{N_w} \left( \frac{D_1}{D_a} \right) \quad (3-44)$$

and

$$\Omega_1 = \left[ \frac{X_{33} + (X_{31} - X_{33})\alpha + \beta(X_{43} + (X_{41} - X_{43})\alpha)}{X_{13} + (X_{11} - X_{13})\alpha + \gamma(X_{23} + (X_{21} - X_{23})\alpha)} \right] \quad (3-45)$$

The mole fraction expression for  $\text{K}^+$  is written as:

$$X_{23} = \Psi_2 \left[ \left\{ X_{23} + (X_{21} - X_{23})\alpha \right\} (\Omega_2)^{1/2} - X_{23} \left\{ \frac{X_{33} + \beta X_{43}}{X_{23} + X_{13}/\gamma} \right\}^{1/2} \right] \quad (3-46)$$

where,

$$\Psi_2 = \frac{\mu_d c}{N_w} \left( \frac{D_2}{D_d} \right) \quad (3-47)$$

and

$$\Omega_2 = \left[ \frac{X_{33} + (X_{31} - X_{33})\alpha + \beta(X_{43} + (X_{41} - X_{43})\alpha)}{X_{23} + (X_{21} - X_{23})\alpha + \gamma^{-1}(X_{23} + (X_{21} - X_{23})\alpha)} \right] \quad (3-48)$$

The mole fraction for  $\text{Cl}^-$  is expressed as:

$$X_{33} = \Psi_3 \left[ \left\{ X_{33} + (X_{31} - X_{33})\alpha \right\} (\Omega_3)^{1/2} - X_{33} \left\{ \frac{X_{13} + \gamma X_{23}}{X_{33} + \beta X_{43}} \right\}^{1/2} \right] \quad (3-49)$$

where,

$$\Psi_3 = \frac{\mu_a c}{N_w} \left( \frac{D_3}{D_a} \right) \quad (3-50)$$

and

$$\Omega_3 = \frac{1}{\Omega_1} \quad (3-51)$$

The mole fraction for the nitrate can be written as:

$$X_{43} = \Psi_4 \left[ \left\{ X_{43} + (X_{41} - X_{43})\alpha \right\} (\Omega_4)^{1/2} - X_{43} \left\{ \frac{X_{13} + \gamma X_{23}}{X_{43} + X_{33}/\beta} \right\}^{1/2} \right] \quad (3-52)$$

where,

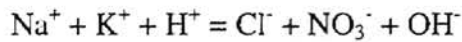
$$\Psi_4 = \frac{\mu_c c}{N_w} \left( \frac{D_4}{D_c} \right) \quad (3-53)$$

and

$$\Omega_4 = \left[ \frac{X_{13} + (X_{11} - X_{13})\alpha + \gamma(X_{23} + (X_{21} - X_{23})\alpha)}{X_{43} + (X_{41} - X_{43})\alpha + \beta^{-1}(X_{33} + (X_{31} - X_{33})\alpha)} \right] \quad (3-54)$$

Using the charge balance equation for the permeate for the system under consideration,

given by Equation (3-21),



and the equilibrium relationship for  $\text{H}^+$  and  $\text{OH}^-$  given by:

$$(\text{H}^+)(\text{OH}^-) = K_w \quad (3-55)$$

the concentrations of  $\text{H}^+$  and  $\text{OH}^-$  can be determined, and hence the pH of the permeate can be obtained.

Expression for Average Mass Transfer Coefficient:

The mass transfer coefficient varies with the ions, and is dependent on the solution viscosity, flow pattern and feed flow rate. Turbulence in the flow channel increases the mass transfer coefficient. The effect of module geometry is taken into consideration by using appropriate expression for the mass transfer coefficient.

Rangarajan et al. (1978a) used the following correlation originally developed by Matsuura et al. (1975).

$$k_i = k_{\text{NaCl}} \left( \frac{D_i}{D_{\text{NaCl}}} \right)^{\frac{2}{3}} \quad (3-56)$$

where  $k_i$  and  $k_{\text{NaCl}}$  are mass transfer coefficient of ion  $i$  and NaCl respectively.  $D_i$  and  $D_{\text{NaCl}}$  are the diffusivity of ion  $i$  and NaCl in water, respectively. The advantage of using the above correlation is that mass transfer coefficient of any ion can be determined if the diffusivities of the ion and NaCl in water are known. The value of  $k_{\text{NaCl}}$  can be determined from the experimental data using Kimura-Sourirajan analysis. The disadvantages of using the above correlation are (i) it does not take into account the geometry of the module and treats the membrane as a flat sheet, and (ii) it needs diffusivity data for the ions and additional experimentation.

Winograd et al. (1973) proposed a mesh step model for electrodialysis system. The model takes in account the spiral-wound geometry of the module, performance of turbulence nets and spacers and hydrostatic conditions dependent on feed flow rates. According to this model, mass transfer coefficient of ions can be calculated as:

$$k_i = \sigma D_i^{2/3} \eta^{-1/6} A_{\text{ch}}^{-1/2} Q_i^{1/2} \quad (3-57)$$

where  $k_i$ ,  $\sigma$ ,  $D_i$ ,  $\eta$ ,  $A_{ch}$  and  $Q_1$  are mass transfer coefficient of ionic species  $i$ , product of mesh step and mixing efficiency of the promoter nets, diffusivity of ion  $i$ , solution kinematic viscosity, area of the feed channel and feed flow rate, respectively. Depending on the availability of the data, either Equation (3-56) or Equation (3-57) can be used to calculate  $k_i$ . Thus the average mass transfer coefficient for the multicomponent system involving four ions can be written as:

$$k_{av} = \frac{\sum_{i=1}^4 k_i}{4} = \frac{k_1 + k_2 + k_3 + k_4}{4} \quad (3-58)$$

#### Material Balances:

Based upon the assumptions of constant molar density and negligible ionic fluxes in comparison to the solvent or water flux, the overall material balance can be written as:

$$Q_1 = Q_2 + M_w N_w A_M \quad (3-58)$$

where  $Q_1$ ,  $Q_2$ ,  $M_w$ ,  $N_w$ , and  $A_M$  are feed flow rate, reject flow rate, molecular weight of water, molar flux of water and area of membrane surface available for the transport, respectively.

The component material balance can be expressed as:

$$Q_1(X_{i1}) = Q_2(X_{i2}) + (M_w N_w A_M)(X_{i3}) \quad (3-59)$$

where  $X_{i1}$ ,  $X_{i2}$  and  $X_{i3}$  are mole fractions of ionic species in the feed, reject and permeate, respectively.

## CHAPTER IV

### MODEL SOLUTION

The multicomponent model described above is applicable to a system with two cations and two anions. The solution to model gives product flux and mole fractions of the ions in the permeate phase, and is obtained by using suitable numerical method. The model equations are highly complex and requires a large set of experimental data. Various essential input parameters, like the permeability constant of water for a particular membrane, solute parameter for NaCl for membrane and mass transfer coefficient for NaCl,  $k_{NaCl}$ , are obtained from Rangarajan et al. (1978a, 1979 and 1984). The input data collected are available for only cellulose acetate membranes. Therefore, the prediction of performance in this thesis is limited to only those types of membranes. The model can be used for other types of membranes if the corresponding input data are provided. The model can be used to evaluate the performance of spiral-wound modules or flat membrane RO units depending on the correlation used for the mass transfer coefficient of the ions. The complete prediction of performance includes:

1. concentration in terms of mole fractions of all the ionic species in the permeate
2. ionic fluxes
3. solvent or water flux
4. recovery, and
5. rejection for all the ions

### Steps involved in the Model Solution

The following input data are available: Composition of the feed, flow rate of the feed, operating gauge pressure, various membrane specifications, diffusivities of ions in water and molar density of the solution. A systematic procedure for obtaining the solution is given below.

1. From literature data (Sourirajan, 1970) on osmotic pressure versus mole fraction of the single salts a, b, c and d, determine  $B_a$ ,  $B_b$ ,  $B_c$  and  $B_d$  for the range of the concentration of interest. Then calculate  $B_{AV}$  from Equation (3-17).
2. Using diffusivity of the ions involved (Parson 1959), calculate  $k_i$  from Equation (3-56) or Equation (3-57) for a flat membrane RO unit or spiral-wound module, respectively.
3. From membrane specification data on solute parameter for NaCl and literature data on free energy parameter for  $\text{Na}^+$  and  $\text{Cl}^-$  ions, calculate  $\ln C_{\text{NaCl}}$  for the membrane using Equation (B-3).
4. Using the value of  $\ln C_{\text{NaCl}}$  and literature data on free energy parameter for the ions involved (Rangarajan et al., 1978a, 1979 and 1984), calculate the solute transport parameters using Equation (B-4).
5. From diffusivity of single salts (Sourirajan 1970) and solute parameters calculated above, determine  $\beta$  and  $\gamma$  from Equations (3-38) and (3-39) respectively.
6. Solve the system of non-linear Equations (3-22), (3-43), (3-46), (3-49) and (3-52) simultaneously using a standard numerical method to obtain solvent flux and mole fractions of the ions in the permeate.



7. Calculate the various ionic fluxes from the Equation (3-42).
8. Calculate recovery and rejection of individual ions using Equation (2-11) and (2-12) respectively.
9. Finally, determine the pH of the permeate by solving Equations (3-21) and (3-55).

### **Description of Computer Code**

The computer code is attached in Appendix C. All the variables used have been defined at the beginning of the code, and a brief description of the purpose of subroutines and the convergence criteria is also given using comment statements in the code. Here, Newton's method for a set of non-linear simultaneous equations using finite difference Jacobian is employed. A detailed description of this numerical method can be found in Kar (1994). To initiate the model solution, an initial guess for five variables, namely, product mole fractions of  $\text{Na}^+$ ,  $\text{K}^+$ ,  $\text{Cl}^-$ ,  $\text{NO}_3^-$  and product flux is required. The product flux for cellulose acetate membranes is usually in the range of 90-1500 gm/hr  $\text{cm}^2$ . For the initial guesses of product mole fractions of above four ions,  $X_{i3}$  is chosen to be 10% of their respective mole fractions in the feed. Since the ionic mole fractions are almost in the same order of magnitude, it is a reasonable way of providing the initial guesses. For the product flux, an arbitrary value is selected from the above given range. The program converges in most of the cases unless the initial guesses are very different from the actual values.

The input and output information is given to DATA file and obtained from OUTPUT file, respectively. The two subroutines, FUNCTN evaluates the functional values, while FUNJAC calculates the elements of the Jacobian matrix using finite

difference method to evaluate the partial derivatives of the functions. The user-supplied derivatives for the functions can be also be used if they are provided. The subroutines LUDCMP and SOLVE do the required matrix manipulations like L-U decomposition and checking if the Jacobian matrix is singular or near singular (Burden and Faires, 1990). The subroutine NEWTON solves the four non-linear equations until the convergence criteria are met.

## CHAPTER V

### RESULTS AND DISCUSSION

The model described in Chapter III is used to predict the performance of RO membranes. The model can be used to for both flat membrane RO units and spiral-wound modules. The range of operating pressures used is between 20 and 120 atmospheres. In all the prediction calculations, the molar density of the solution was assumed to be that of pure water, and osmotic pressure versus mole fraction correlation was approximated to be a straight line in the range of concentration used for calculation of  $B_{AV}$ . The area of membrane surface available for the transport in a flat membrane RO unit is assumed to be  $5000 \text{ cm}^2$ . Diffusivity data of ions at  $25^\circ\text{C}$  are obtained from Parsons (1959), and is given in the Table II. The data on free energy parameters of different ions required to calculate solute transport parameters for single salts are collected from Matsuura et al. (1975), and is also given in Table II. In all the cases, a flow rate of  $400 \text{ cm}^3/\text{min}$  is assumed, and temperature of operation is maintained at  $25^\circ\text{C}$ . In this analysis, cellulose acetate membranes with  $\text{Na}^+$ ,  $\text{K}^+$ ,  $\text{Cl}^-$  and  $\text{NO}_3^-$  ions are selected. Similar analysis for other types of membranes and a different set of four ions can be done if the appropriate input data are available. The essential data pertaining to the different cellulose acetate membranes with varying surface porosities used in the prediction is given in the Table III (Rangarajan et al., 1978a). For spiral-wound modules, the mass

transfer coefficient based on Winograd et al. (1973) is used, with the following arbitrary assumptions:

(i) Product of mesh-step and mixing efficiency of a turbulence promoter net,

$$(\sigma) = 0.7$$

(ii) Total area of membrane surface available for membrane transport,

$$(A_M) = 1000 \text{ cm}^2$$

(iii) Area of feed channel ( $A_{ch}$ ) =  $50 \text{ cm}^2$

The non-linear equations of the model are solved by a computer code using Newton's method for non-linear simultaneous equations with a finite difference Jacobian. A detailed description of the numerical method can be found in Kar (1994).

Some experimental results on ion separation and product rates for the system involving  $\text{Na}^+$ ,  $\text{K}^+$ ,  $\text{Cl}^-$  and  $\text{NO}_3^-$  are available in Rangarajan et al. (1978a). The model was used for the same experimental conditions with the same type of cellulose acetate membranes. A comparison of the predicted and experimental results on ion-separation and product fluxes is given in Table IV, and is found to be in fairly good agreement.

Table II: Free Energy and Solute Transport Parameters of Ions

Ions	$-\Delta\Delta G/RT$	$D_i \times 10^5 (\text{cm}^2/\text{sec})$
$\text{Na}^+$	5.79	1.35
$\text{K}^+$	5.91	1.98
$\text{Cl}^-$	-4.42	2.03
$\text{NO}_3^-$	-3.66	1.92

Table III: Specifications of Different Cellulose Acetate Membranes

Membrane or Film No.	$A \times 10^6$	$\mu_a \times 10^5$ (cm/s)	$\mu_c \times 10^5$ (cm/s)	$\mu_d \times 10^5$ (cm/s)	$-\ln C_{NaCl}$	$k_{NaCl} \times 10^5$ (cm/sec)
1	0.593	7.1	15.2	8.03	10.92	13.7
2	1.353	123.1	263.2	138.7	8.07	20.8
3	1.446	174.7	373.5	196.9	7.72	21.6
4	1.531	9.8	88.5	46.66	9.16	22.4
5	1.287	848.0	1813.3	956.2	6.14	38.1
6	0.946	9.4	22.5	10.62	10.64	17.0
7	1.127	1077.0	2436.2	1215.5	5.9	18.7

The model was tested using various CA membrane specifications for different operating and feed conditions. The results are systematically presented in the foregoing discussion. The mixed solute feed of NaCl and KNO<sub>3</sub> with the following three different compositions over a range of concentration was considered. The operating conditions and the membrane specifications used were the same in all three cases. The input parameters are given in Table V.

Feed-I: 10000 ppm of NaCl + 9000 ppm of KNO<sub>3</sub>

Feed-II: 4500 ppm of NaCl + 3000 ppm of KNO<sub>3</sub>

Feed-III: 300 ppm of NaCl + 400 ppm of KNO<sub>3</sub>

The model was used to predict the performance of the membrane for the above mentioned three different feed concentrations. The results of prediction are presented in Table VI. The ion separation and product flux for the all the three cases is observed to vary significantly. The actual performance of any particular membrane with respect to a

Table IV: Comparison of Experimental and Predicted Results

	Film No.	Product Flux (gmoles/cm <sup>2</sup> -sec)	Product Mole Fractions			
			Na <sup>+</sup>	K <sup>+</sup>	Cl <sup>-</sup>	NO <sub>3</sub> <sup>-</sup>
Experimental	1	7.92E-06	0.01675	0.004	0.01595	0.00481
Predicted	1	7.98E-06	0.01532	0.00361	0.01497	0.00366
Experimental	2	7.01E-05	0.01576	0.01687	0.01351	0.01912
Predicted	2	6.54E-05	0.01463	0.01641	0.01453	0.01632
Experimental	3	9.76E-05	0.00672	0.03882	0.00543	0.04011
Predicted	3	8.16E-05	0.00612	0.03295	0.00584	0.03302
Experimental	4	7.18E-05	0.00233	0.00175	0.00176	0.00232
Predicted	4	6.72E-05	0.00229	0.00157	0.00121	0.00247
Experimental	5	2.09E-05	0.00335	0.00514	0.00307	0.00542
Predicted	5	1.81E-05	0.00319	0.00465	0.00272	0.00479

Table-V: Common Input Data for the Three Feed Compositions of NaCl and KNO<sub>3</sub>

Property	Value
Membrane permeability constant, (gmole of H <sub>2</sub> O/cm <sup>2</sup> s atm), $A \times 10^5$	0.946
$\mu_a \times 10^5$ (cm/s)	9.4
$\mu_b \times 10^5$ (cm/s)	22.3
$\mu_d \times 10^5$ (cm/s)	10.62
$-\ln C_{NaCl}$	10.64
$k_{NaCl} \times 10^4$ (cm/s)	17.0
Operating pressure (atm)	68.0
Temperature (°C)	25.0
Feed flow rate (cm <sup>3</sup> /s), $Q_1$	400.0
Molar density (gmol/cm <sup>3</sup> ), $c \times 10^2$	5.4
$B_{AV}$ (atm)	1100.0
Area of membrane surface (cm <sup>2</sup> )	5000.0

Table VI: Prediction of Membrane Performance for Three Different Feed Conditions

Property	Feed I	Feed II	Feed III
Mole fractions in permeate			
Na <sup>+</sup>	4.986E-04	2.063E-04	1.445E-05
K <sup>+</sup>	3.329E-04	1.021E-04	1.444E-05
Cl <sup>-</sup>	3.721E-04	1.654E-04	9.371E-06
NO <sub>3</sub> <sup>-</sup>	4.432E-04	1.398E-04	1.124E-05
Ionic Fluxes(gmole/cm <sup>2</sup> s)			
Na <sup>+</sup>	2.466E-08	1.189E-08	9.238E-10
K <sup>+</sup>	1.646E-08	5.882E-09	9.201E-10
Cl <sup>-</sup>	1.840E-08	9.537E-09	5.972E-10
NO <sub>3</sub> <sup>-</sup>	2.215E-08	8.132E-09	7.129E-10
Water Flux(gmole/cm <sup>2</sup> s), N <sub>w</sub>	4.945E-05	5.763E-05	6.373E-05
Permeate Flow(cm <sup>3</sup> /s), Q <sub>3</sub>	267.1	311.2	344.1
Reject Flow(cm <sup>3</sup> /s), Q <sub>2</sub>	132.9	88.8	55.9
Recovery(%), Y	66.8	77.8	86.1
Rejection of ions			
Na <sup>+</sup>	83.9	85.1	85.8
K <sup>+</sup>	80.4	81.8	82.4
Cl <sup>-</sup>	88.0	88.0	90.1
NO <sub>3</sub> <sup>-</sup>	72.8	74.1	74.4
pH of the permeate	8.97	8.74	8.33



given solution system depend not only on the osmotic pressure of the feed solution but also on the physical and chemical nature of the membrane. According to Kimura-Sourirajan analysis, the basis for this model, when the size of the pores on the membrane surface is only a few times larger than the size of the permeating molecules, the transport of the solvent water through the porous membrane is proportional to the effective pressure, and of the solute is due to pore diffusion and hence proportional to its concentration difference across the membrane. Therefore, it can be seen from the Table VI that the ion separation for  $\text{Na}^+$ ,  $\text{K}^+$ ,  $\text{Cl}^-$  and  $\text{NO}_3^-$  increases with the dilution of the feed. At constant pressure, as the feed concentration decreases, the concentration difference across the membrane decreases and the permeate of higher quality is obtained. Although the difference in the percentage rejection for all the four ions is not high between Feed I, Feed II and Feed III, it is significant enough to explain the trend that can be observed with any RO membrane.

The solute parameters,  $\mu_a$  and  $\mu_b$  for  $\text{NaCl}$  and  $\text{KNO}_3$ , play a role of mass transfer coefficient with respect to ionic transport through the membrane. They are treated as a single quantity for the purpose of analysis. Actually, the solute transport parameter is not a single factor, but a combination of several inter-related factors, none of which are precisely known for chemical engineering calculations. The difference in the value of  $\mu$  for  $\text{NaCl}$  and  $\text{KNO}_3$  for the membrane used offers a method of explaining membrane selectivity for those salts. Hence it is used to illustrate the relative levels of ionic separation and product rate for  $\text{NaCl} + \text{KNO}_3$  system. A higher value of solute transport parameter usually implies a lower level of solute separation; but the order of solute

separation with respect to any two salts does not always correspond to the order of their values of solute transport parameter. The values of  $\mu$  for most inorganic and organic solutes at constant pressure are independent of concentration of feed, concentration at boundary layer, and feed flow rate. From the Table V,  $\mu$  for  $\text{KNO}_3$  is higher than  $\mu$  for  $\text{NaCl}$ , and therefore, ionic separation for  $\text{K}^+$  and  $\text{NO}_3^-$  are lower than  $\text{Na}^+$  and  $\text{Cl}^-$  for all the three feed systems.

The permeability constant  $A$ , and  $\mu$  depend on the porous structure of the membrane; and hence, they are different for different membranes. The number of pores and pore size distribution on the membrane surface can be expected to affect ionic separation. The quantity  $A$  is a measure of the overall porosity of the membrane in terms of permeation rate of pure water, and is independent of any solution under consideration, feed concentration and feed flow rate. From the results presented in the Table VI, recovery or the percentage of the feed converted to permeate, increases with the decrease of feed concentration. The recovery increases from 66.8% for Feed I to 86.1% for Feed III. This can be explained as increase in feed concentration increases the osmotic pressure of the solution resulting in decrease of effective driving force for the water flow.

The mass transfer coefficient  $k$ , plays a vital role in ionic separation and represents the concentration polarization on the higher pressure side of the membrane. The mass transfer coefficient is primarily dependent on feed flow rate, feed concentration and module geometry. The experimental data available in the literature indicates that  $k$  is a weak function of pressure, therefore, its dependence on pressure can be neglected. For the system of  $\text{NaCl} + \text{KNO}_3$ , the correlation for variation of mass transfer coefficient with

feed concentration could not be obtained. Hence, an average value of  $k$  was used for all the three cases.

The preceding discussion on the prediction of performance pertains to a flat membrane RO unit. Since the difference between the prediction of performance for a spiral-wound module and a simple flat RO unit exists only in the expression for the mass transfer coefficient, a similar discussion can be applicable to the performance of spiral-wound modules.

Figure 2 illustrates the effect of operating pressure on the product flux of a cellulose acetate RO membrane. The feed consists of 1000 ppm NaCl + 1000 ppm  $\text{KNO}_3$  and uses the membrane film-7 from the Table III. Under constant feed conditions, the applied pressure is varied till 120 atm, which is generally considered to be the practical limit for the pressure applied in reverse osmosis operations. The permeate flux increases with the increase of applied pressure. This is because the effective driving force for the water flow increases with the increase of pressure across the membrane. The product flux is zero at about 28 atm, and this corresponds to the minimum applied pressure that is required to overcome osmotic pressure difference across the membrane to produce flux. The minimum applied pressure depends on the concentration of the feed; the higher the concentration of the feed, the more is the minimum applied pressure to produce flux.

The effect of increase in operating pressure on ionic separation for flat-membrane RO unit and a spiral-wound module is shown in the Figures 3 and 4, respectively. The concentrations of NaCl and  $\text{KNO}_3$  in the feed are 2.50 m and 0.48 m, respectively. The membrane film-1 in the Table III is used for this particular system. The mole fractions of

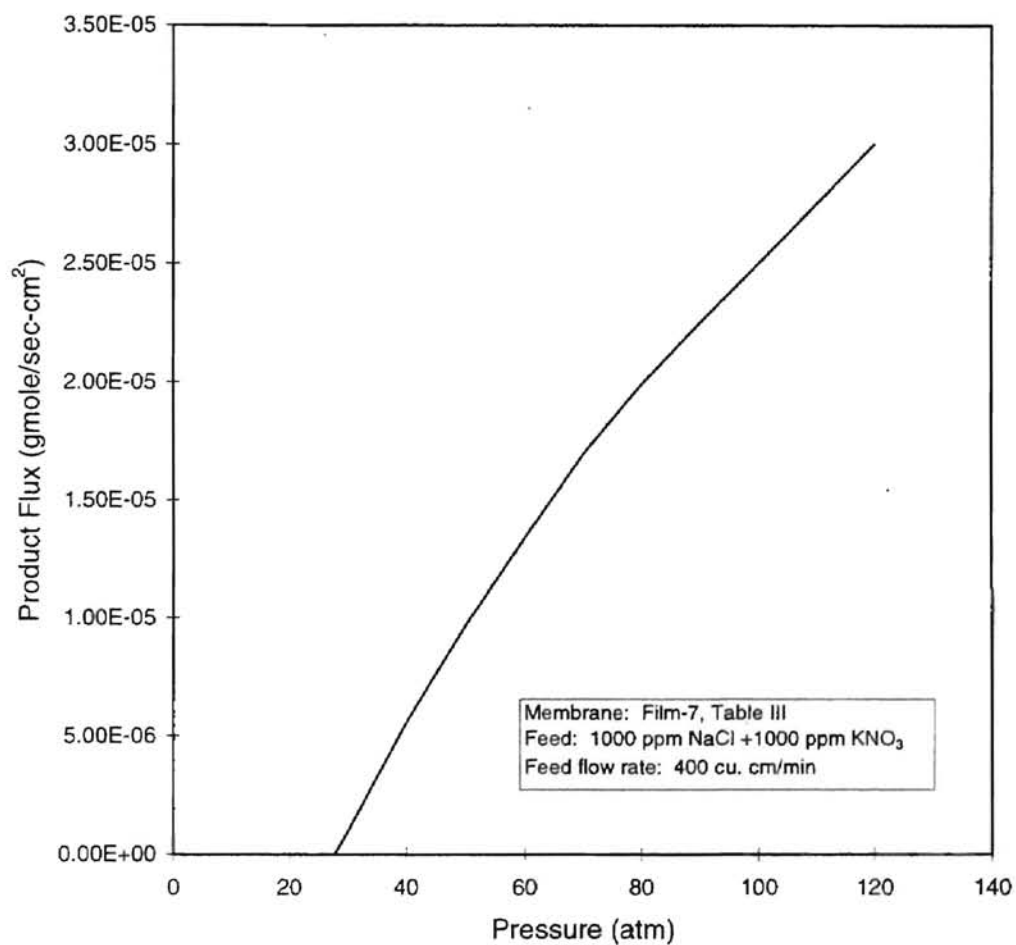


Figure 2: Effect of Operating Pressure on Product Flux.

(Flat-Membrane RO Unit)

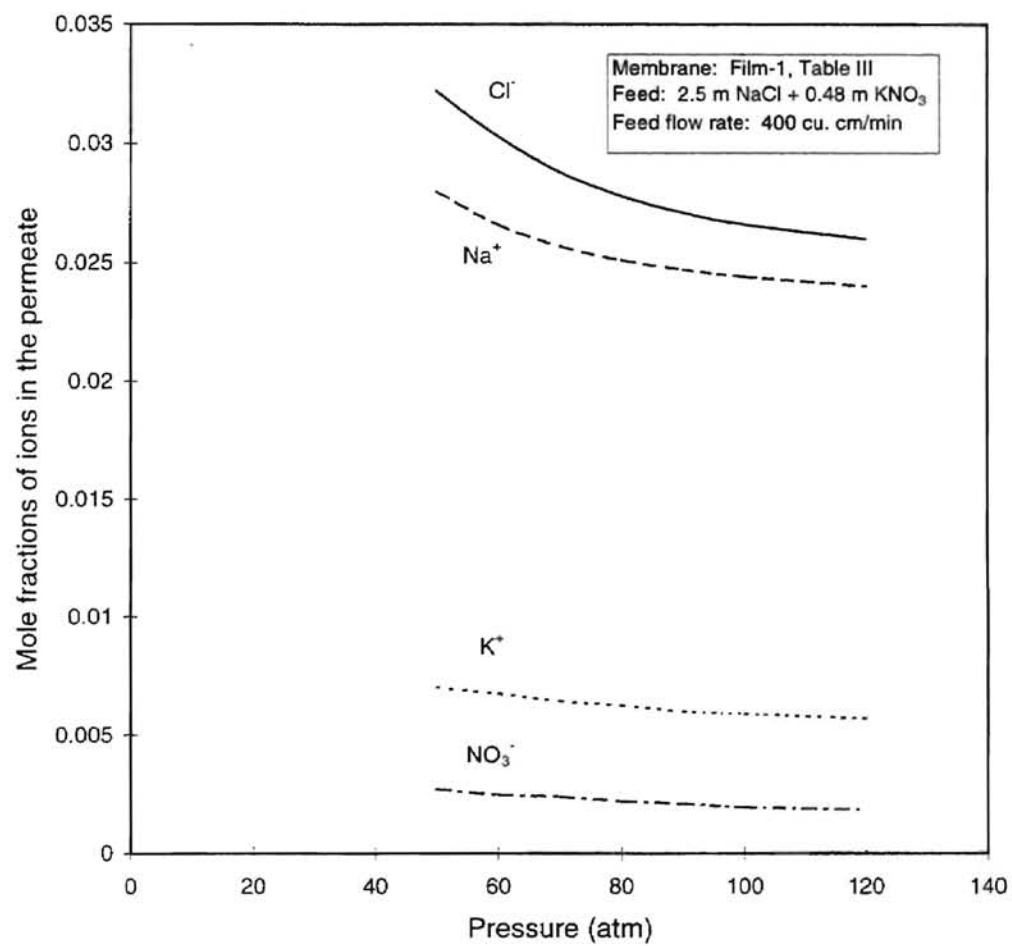


Figure 3: Effect of Operating Pressure on Product Mole Fractions.  
(Flat-Membrane RO Unit)

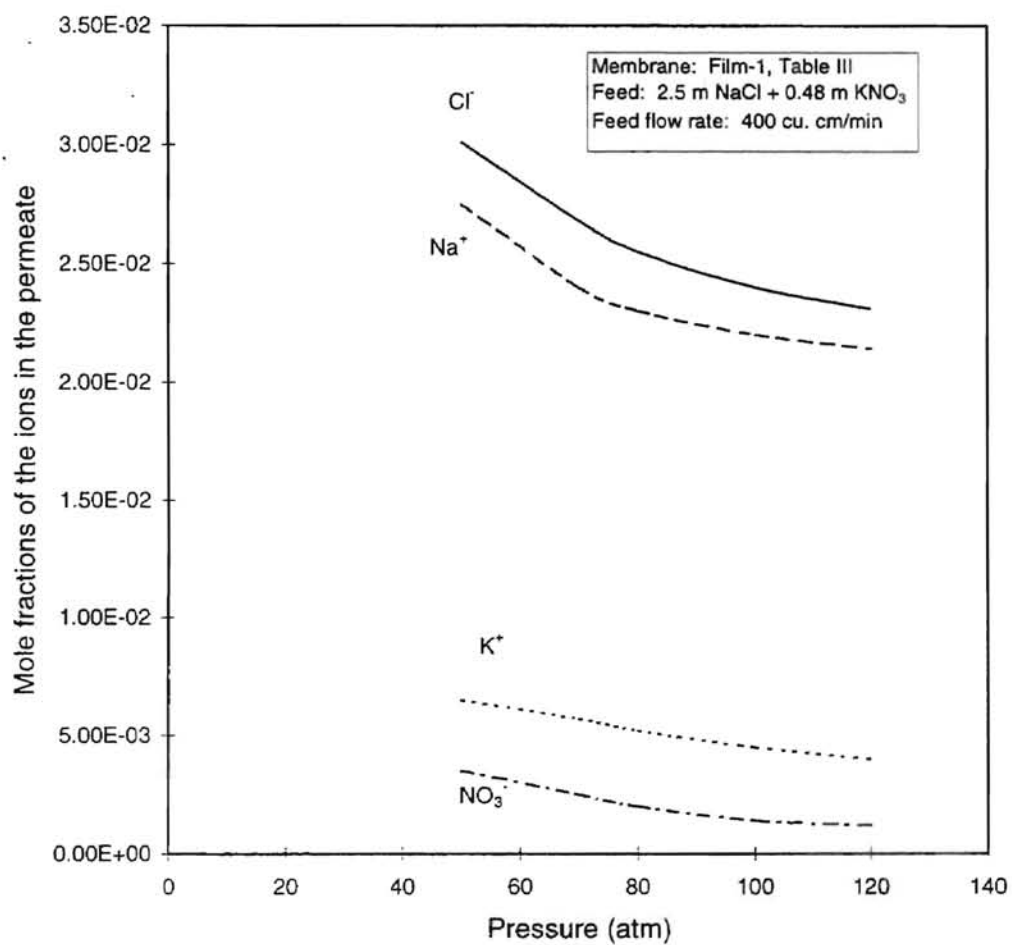


Figure 4: Effect of Operating Pressure on Product Mole Fractions.  
(Spiral-Wound Module)

$\text{Na}^+$ ,  $\text{K}^+$ ,  $\text{Cl}^-$  and  $\text{NO}_3^-$  in the product decrease with the increase in pressure. This rise in the product quality is due to an increase in preferential sorption of the membrane for pure water at higher pressures, and also could be due to decrease in the average pore size on the membrane surface with the increase in pressure. Figures 5 and 6 show the variation of pH of the permeate with the above operating conditions for a Flat-membrane RO unit and a spiral-wound module respectively. A slight pH change from about 4 to 2 is observed in both the cases, and this accounts for the slight variation in the fluxes of the different ions over the range of applied pressure. Figure 7 shows the effect of operating pressure on the product flux of a spiral-wound module with the above feed conditions and membrane specifications.

Figures 8 and 9 show the effect of feed concentration on the concentration of ions in the permeate for flat-membrane RO unit and spiral wound module, respectively. In both the cases, operating pressure is constant and maintained at 100 atm. The membrane specifications are that of film-1 in the Table III. While the concentrations of  $\text{Na}^+$  and  $\text{Cl}^-$  ions are same in the feed solution for both the cases, they are different in the product as a result of reverse osmosis; such is also the case with respect to the relative concentrations of  $\text{K}^+$  and  $\text{NO}_3^-$  ions. The relative concentration of each ion in the product from a simple RO unit or spiral-wound module is a function of both feed composition and membrane specifications. The mole fractions of  $\text{Na}^+$  and  $\text{Cl}^-$  in the product solution increases with an increase in their concentration in the feed solution, and the mole fractions of  $\text{K}^+$  and  $\text{NO}_3^-$  decreases with a decrease in their concentration in the feed solution. As the

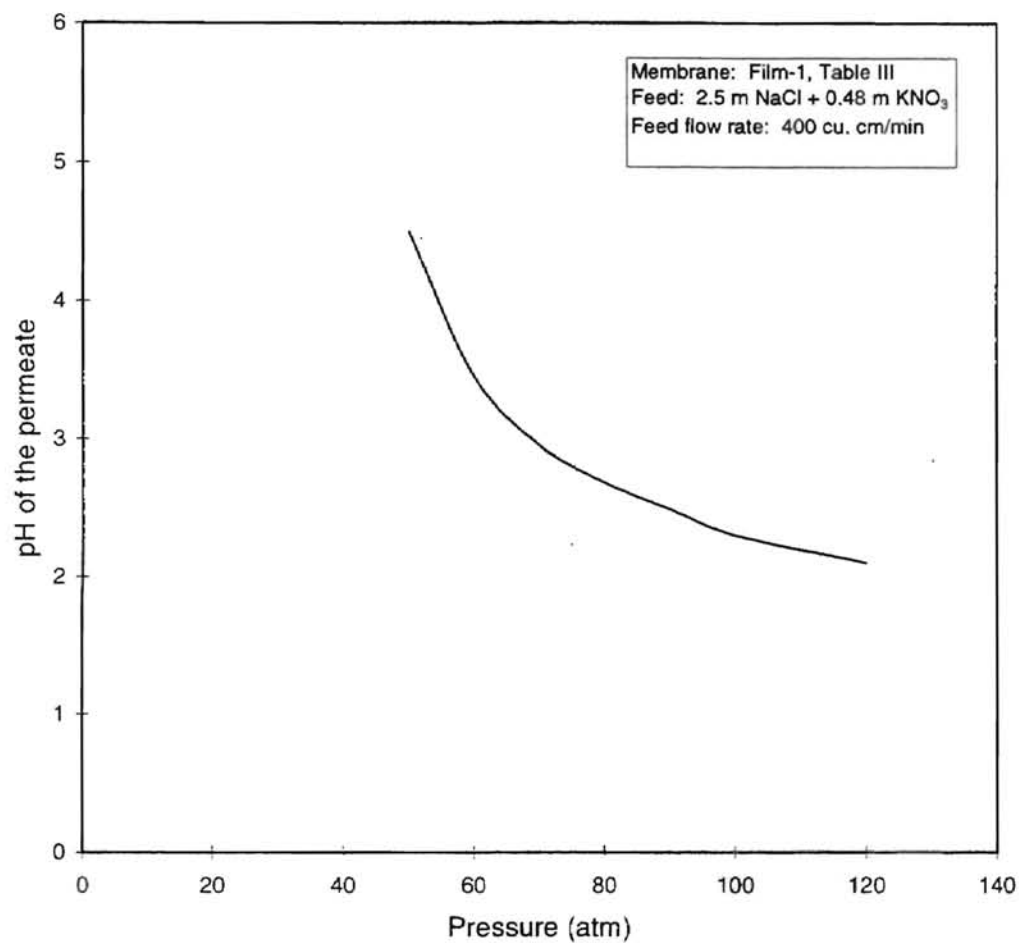


Figure 5: The Variation of pH of the Permeate.

(Flat-Membrane RO Unit)



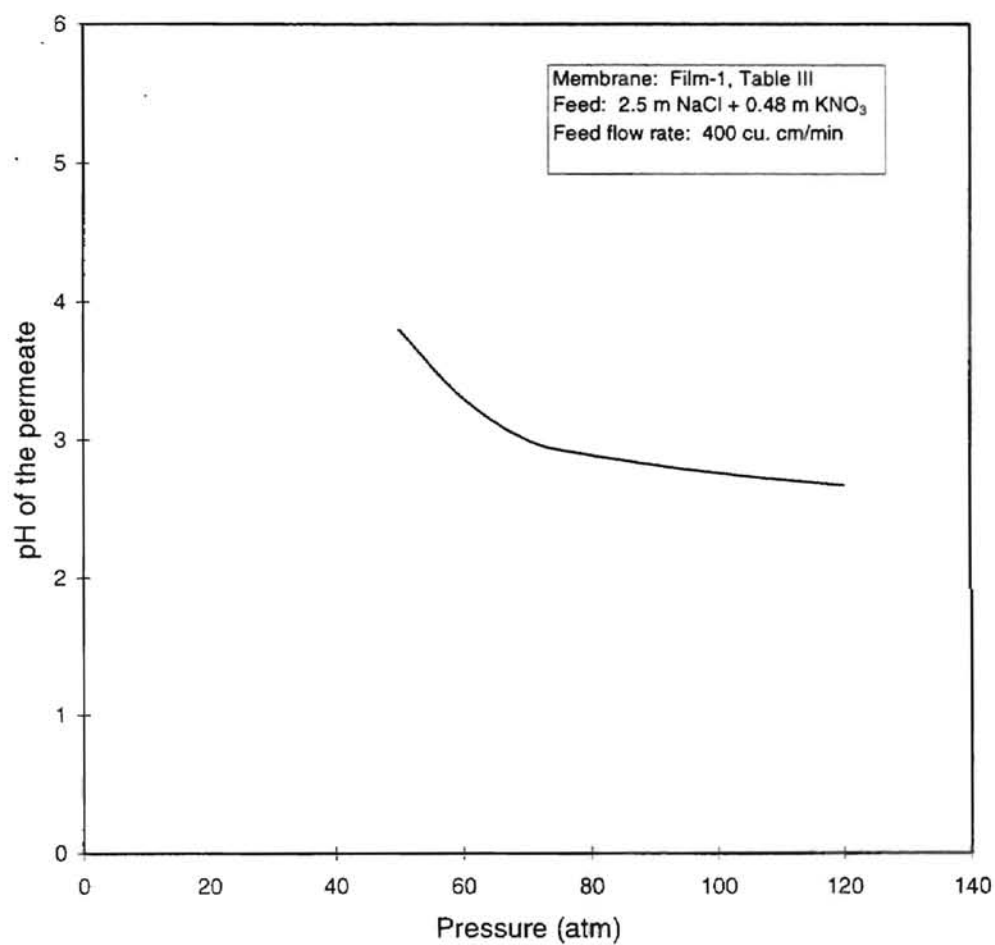


Figure 6: The Variation of pH of the Permeate.  
(Spiral-Wound Module)

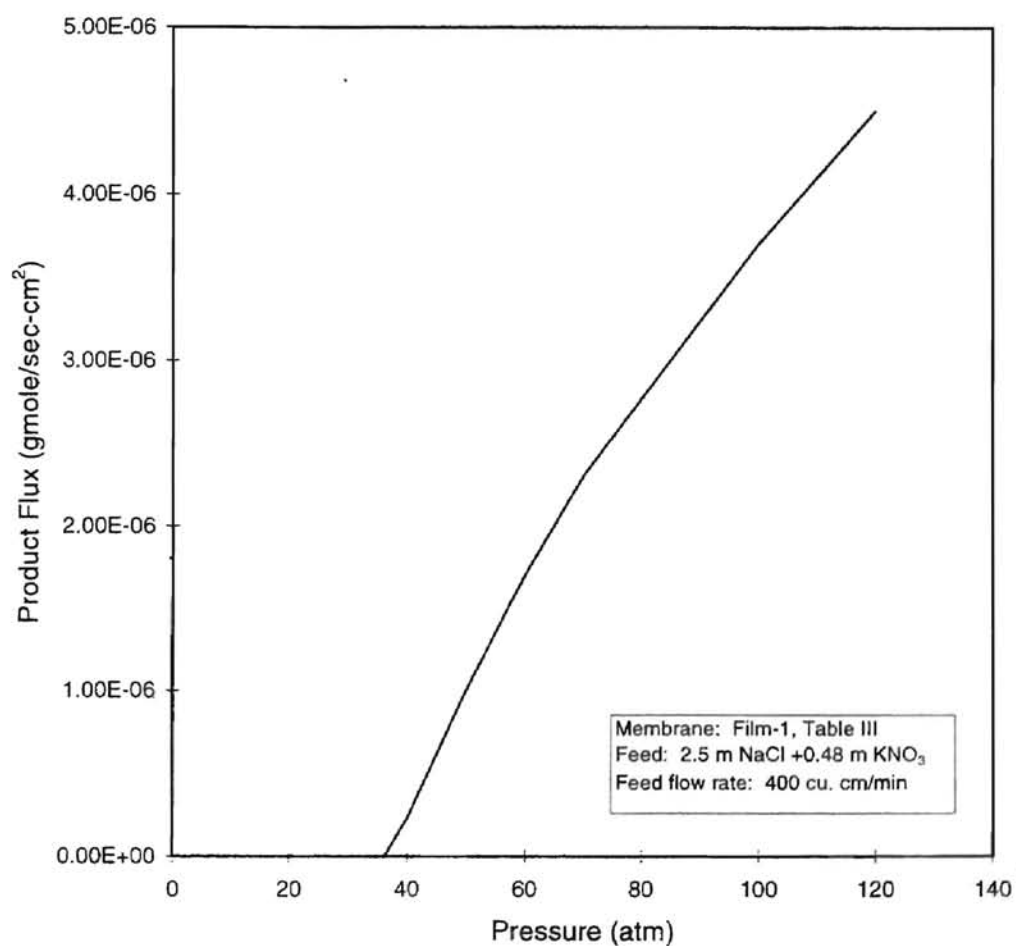


Figure 7: Effect of Operating Pressure on Product Flux.

(Spiral-Wound Module)

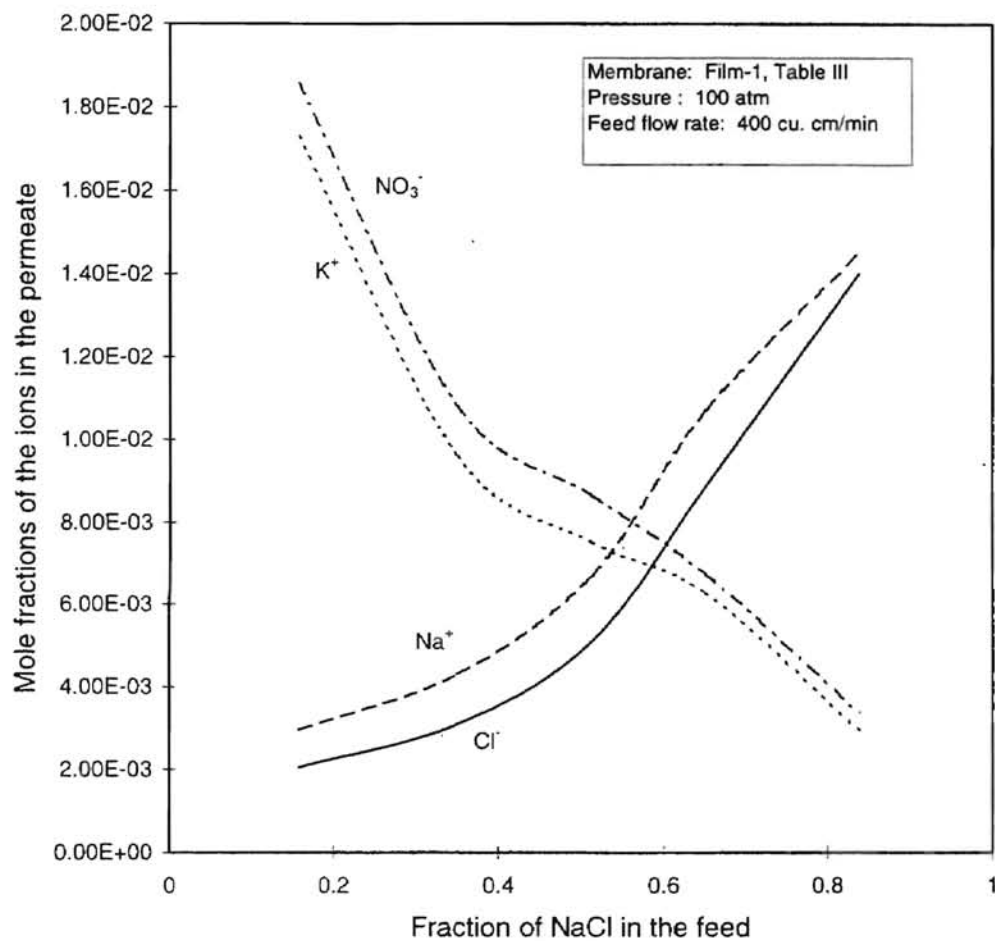


Figure 8: Effect of Feed Concentration on Product Mole Fractions of Ions.

(Flat-Membrane RO Unit)

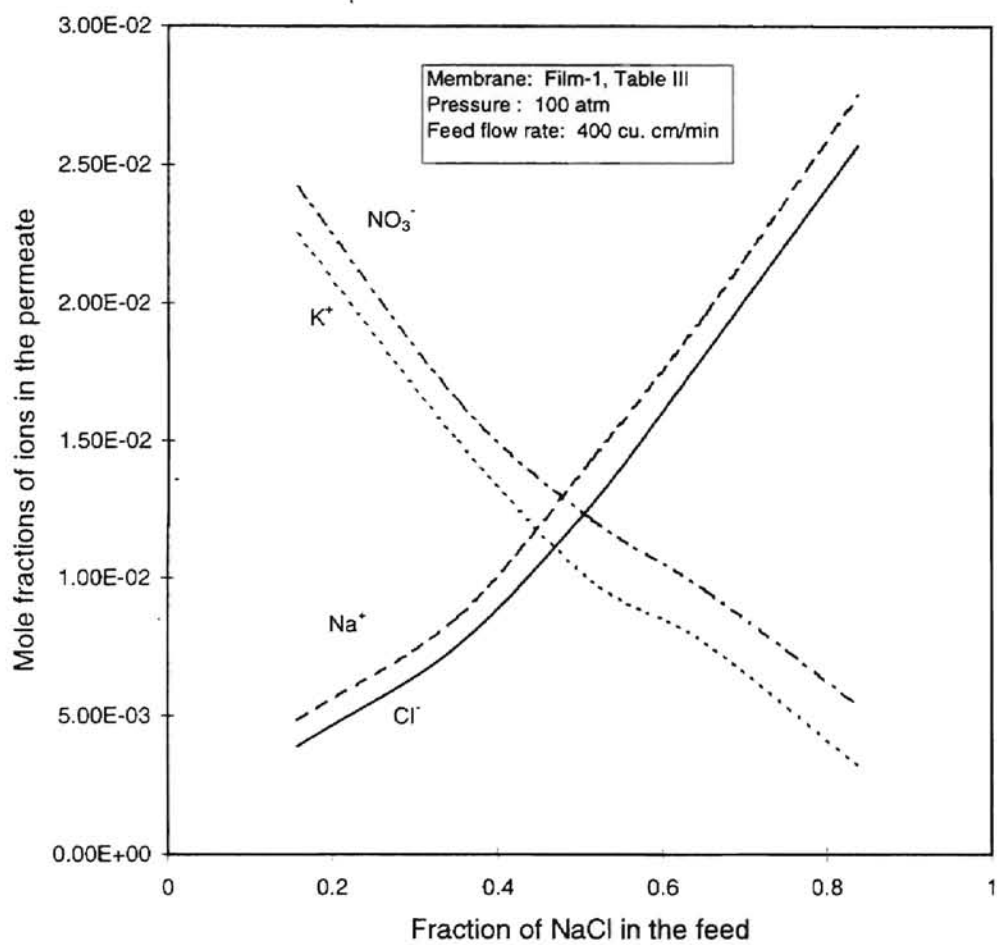


Figure 9: Effect of Feed Concentration on Product Mole Fractions of Ions.  
(Spiral-Wound Module)

concentration of the feed rises, the concentration difference across the membrane increases, thereby increasing the solute transport and vice versa. The difference in the permeate concentrations between the flat-membrane RO unit and spiral-wound module for the same operating conditions and membrane specifications is because of different module designs and different mass transport characteristics.

Figures 10 and 11 show the effect of mass transfer coefficient  $k_{av}$  on the high pressure side of the membrane film-7 for the feed system of 4500 ppm NaCl and 3000 ppm  $KNO_3$  at the applied pressure of 60 atm. The results indicate that both percentage ion separation and product rate increase with increase in  $k_{av}$  especially upto the  $70 \times 10^{-4}$  cm/s and then attain approximately constant values. The increase in mass transfer coefficient due to increase in turbulence results in decrease of concentration polarization at the membrane surface, and thus facilitates the solute and solvent transport across the membrane. Beyond a certain value of  $k_{av}$ , corresponding to the maximum turbulence or near zero concentration polarization conditions, the performance of the membrane cannot be improved further by a mere increase in mass transfer coefficient.

Unlike the expression for mass transfer coefficient for a simple RO unit, the correlation of  $k$  for spiral-wound unit given by Equation (3-57), contains the feed flow rate term  $(Q_1)$ , and is directly proportional to the  $(Q_1)^{1/2}$ . So the effect of feed flow rate on the permeate quality can be observed with the spiral-wound module.

Figures 12 and 13 illustrate the effect of feed flow rate on the ion separation and water flux of a spiral wound module with membrane film-6 of Table III using feed composition of 4500 ppm NaCl + 10000 ppm  $KNO_3$  at pressure equal to 60 atm. The ionic mole fractions in the permeate drop or the ionic separation rises with the rise in feed

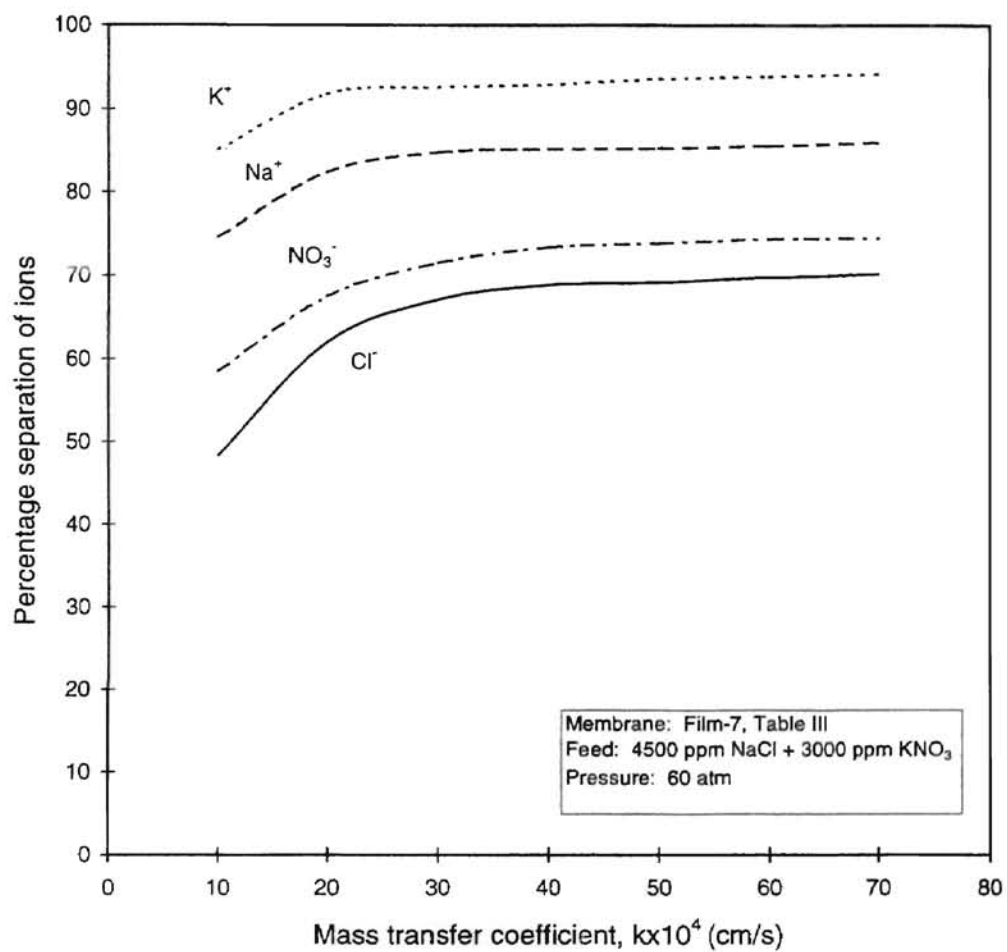


Figure 10: Effect of Increase in Mass Transfer Coefficient on Ion Separation.

(Flat-Membrane RO Unit)

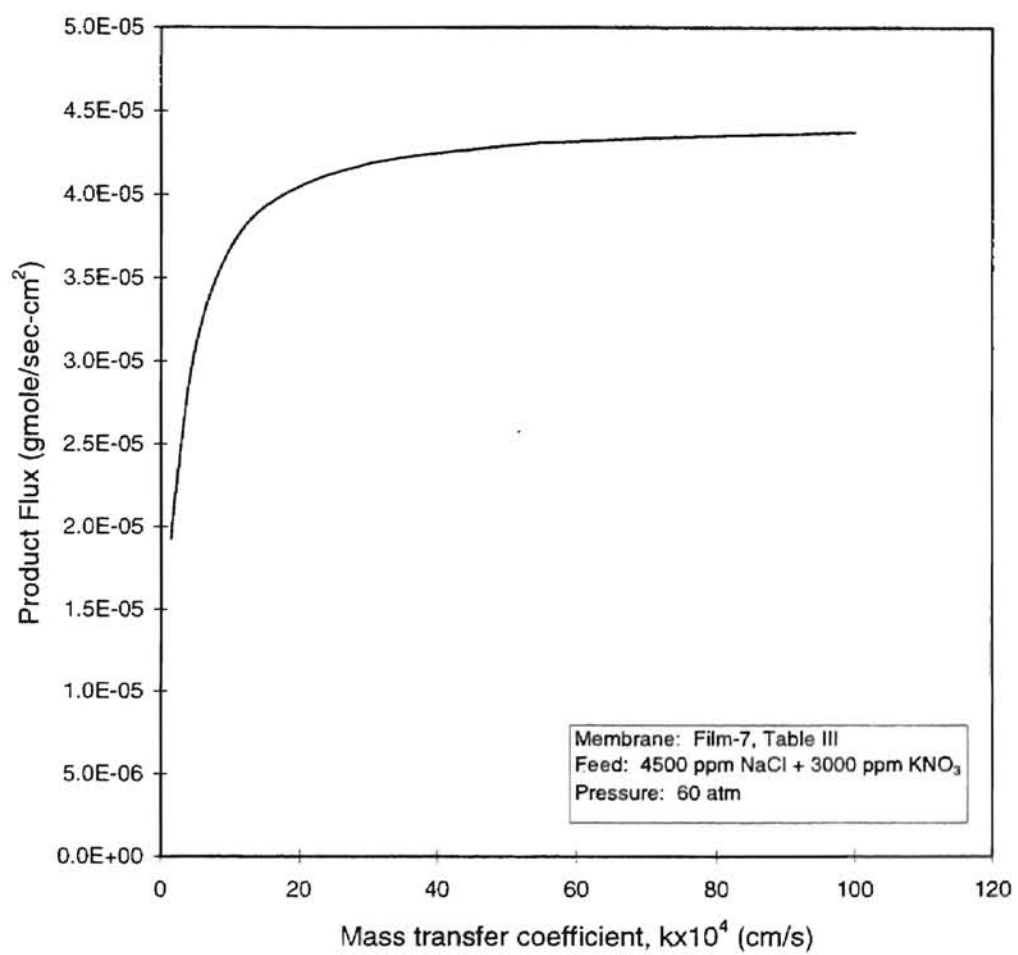


Figure 11: Effect of Increase in Mass Transfer Coefficient on Product Rate.

(Flat-Membrane RO Unit)

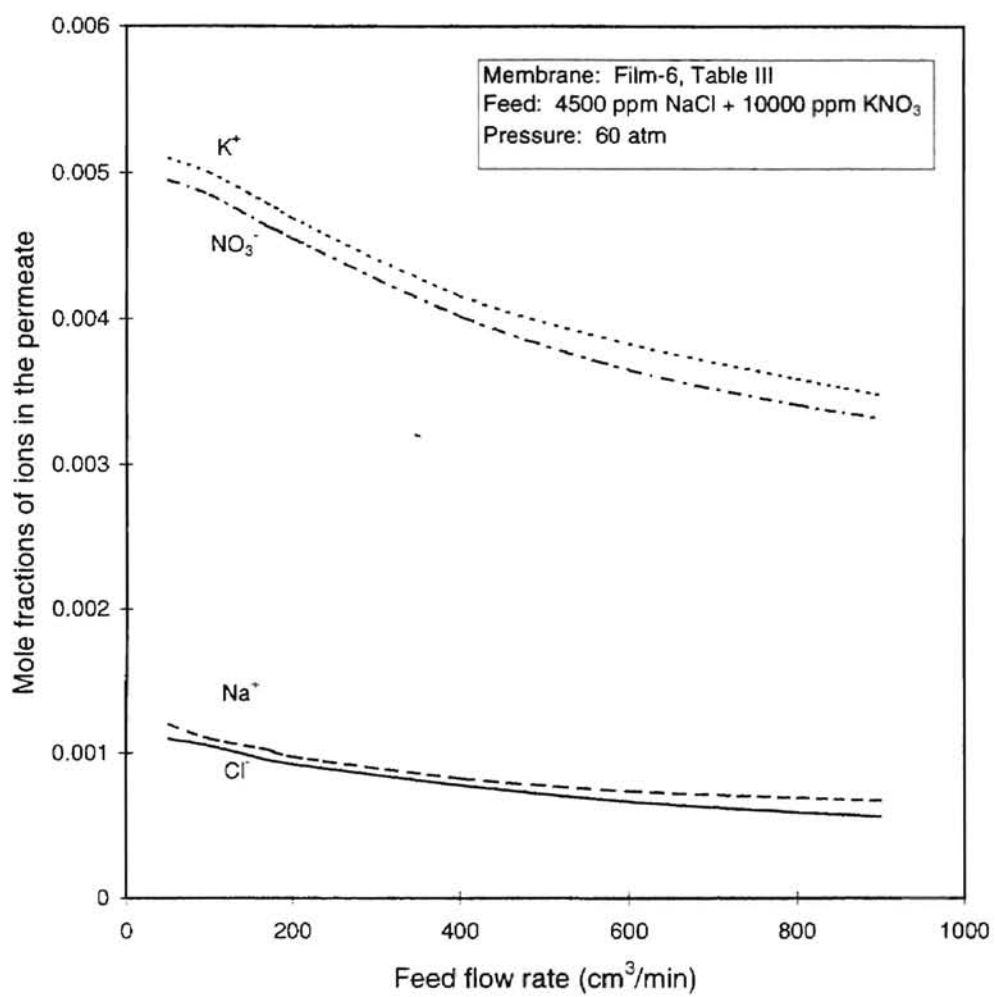


Figure 12: Effect of Feed Flow rate on Rejection of Ions in a Spiral-Wound Module.



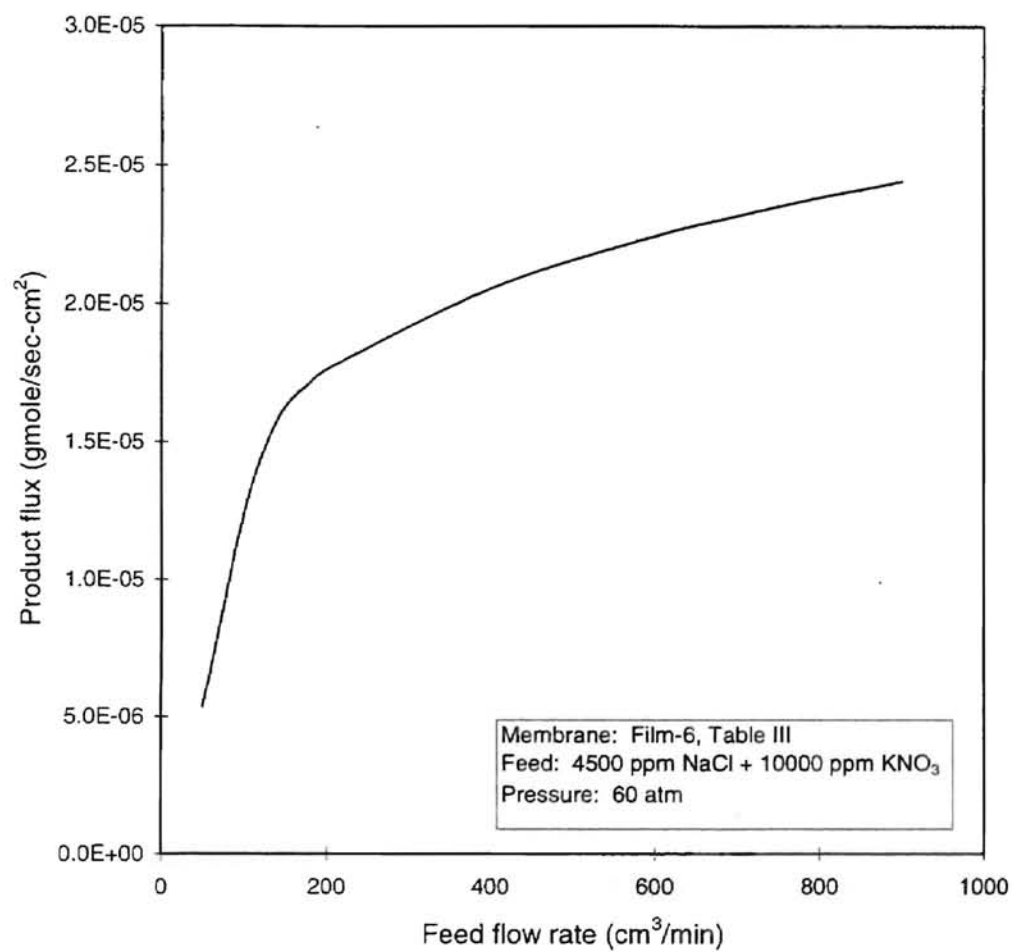


Figure 13: Effect of Feed Flow Rate on Product Flux of a Spiral-Wound Module.

flow rate, and flux increases with the increase in feed flow rate, thereby producing a product of better quality. The increase in feed flow imparts a higher degree of turbulence, reduces the concentration built up at the vicinity of membrane surface, and promotes better ionic separation and enhances the recovery.

## **CHAPTER VI**

### **SEPARATION OF AMINES USING PERVAPORATION**

#### **Introduction**

As mentioned in Chapter II, pervaporation is a membrane process characterized by the presence of membrane barrier between a liquid and a gaseous phase, with mass transfer occurring selectively across the barrier to the gas side. Since it involves permeation of solute through the membrane followed by evaporation, it is conveniently called pervaporation. Over the past few years, pervaporation has gained acceptance by the industry as an effective process for separation and recovery of organic mixtures. Currently, its best application is in the dehydration of aliphatic alcohols from aqueous mixtures. The driving force for pervaporation is chemical potential gradient or concentration difference across the membrane. The selectivity of membrane is the determining factor in the relative separation of different components present in the liquid phase. In addition to inherent advantages of a membrane process, nonporous nature of the membrane makes the process less susceptible to degradation or fouling. In contrast to reverse osmosis, the osmotic pressure is not limiting, because the permeate, which is in gaseous phase, is maintained at very low pressure.

The transport through nonporous membrane in pervaporation is described by widely accepted solution-diffusion mechanism (Binning et al., 1961). According to this mechanism, the three steps involved are (Fleming and Slater, 1990):

1. Sorption of liquid mixture on the high pressure or feed side of the membrane
2. Diffusion through the membrane
3. Desorption of liquid mixture on the low pressure or gaseous side of the membrane

A thorough discussion of transport theory and models for pervaporation can be found in Aptel and Neel (1986).

### **Pervaporation Experiments for Amine Separation**

The purpose of this chapter is to provide some qualitative insight into amine separation from pure aqueous mixtures and from aqueous mixtures in the presence of inorganic salts like NaCl using pervaporation process. Some experiments were conducted with the systems of Ethanolamine (ETA) and Water, ETA and NaCl in the Water, and Dimethylamine and Water using Nafion membrane ( $K^+$  form). The objective of the experimentation was to investigate the possibility of amine separation with pervaporation.

The experiments were carried out with the pervaporation apparatus designed by Kamal (1995). The schematic of experimental setup is given in Figure 9. The most important part of the whole process is pervaporation cell where the actual process takes place. All lines are made of 0.25 inch stainless steel pipes except the coil in water bath which is made of copper for better conduction of heat. All lines are connected with Swagelok fittings. The feed mixture of known composition is fed to the feed tank. The feed circulates through the coils of the waterbath. After attaining the desired temperature in the water bath, the feed passes through the membrane cell where it undergoes pervaporation process. The reject is recycled to the feed tank and the permeate is drawn

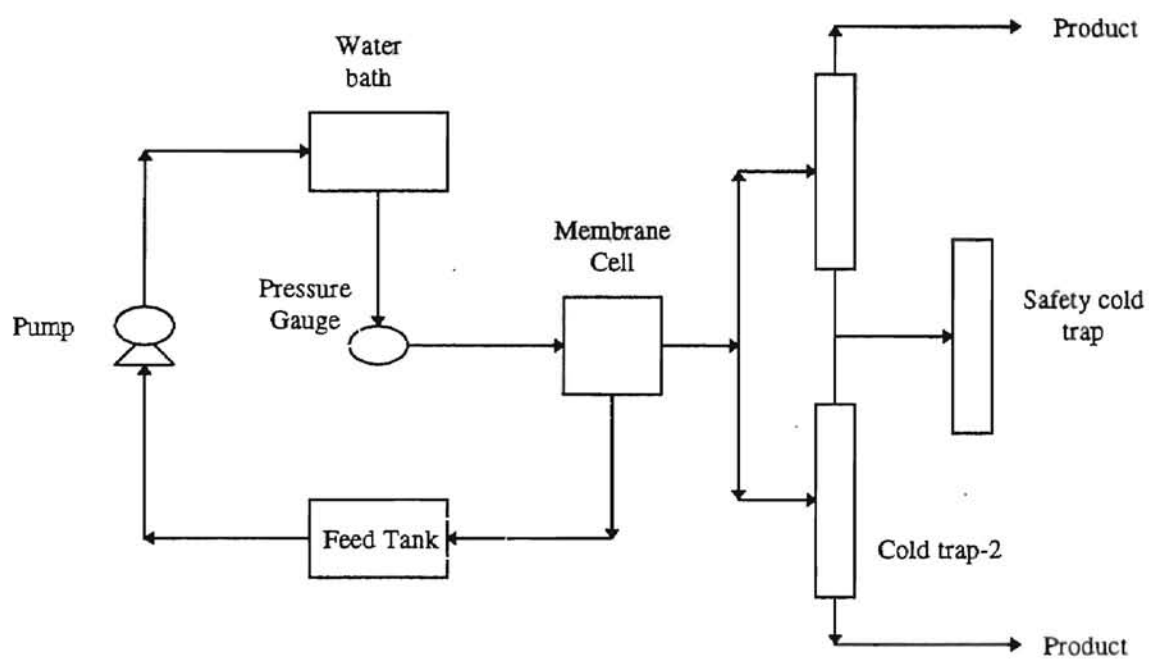


Figure 14: Experimental Setup of the Pervaporation Apparatus.

under vacuum and is collected in cold traps where it is condensed using liquid nitrogen or freezing mixture made of dry ice and acetone.

In order to make the process continuous, the two cold traps are used alternately. While one cold trap is in operation, the other one is vented for product collection and made ready for subsequent operation. The outlets from these two product cold traps are connected to a third liquid nitrogen cold trap to prevent permeate from reaching the vacuum pump and also to prevent vacuum pump oil from entering the product cold traps when the equipment is switched off. The membrane is held in place using two Teflon O-rings and a stainless support gauze. The effective area available for transport is 45 cm<sup>2</sup>. The membrane cell is mounted on a tripod stand and is made leak-proof.

The amine separation for the following compositions of feed were investigated and repeated to obtain reproducible results.

Feed-I: Water + approximately 5 ppm Ethanolamine

Feed II: Water + approximately 5 ppm Dimethylamine

Feed III: Water + approximately 5 ppm ETA + 43 ppb Na + 56 ppb Cl

All the experiments were conducted at a constant feed temperature of 40°C, for about 6 hours of uninterrupted operation with Nafion membrane. The feed flow rate was maintained at about 10.2 cm<sup>3</sup>/s by adjusting the reject flow rate, and the product rate was found to be around 0.000014 cm<sup>3</sup>/s in almost all the cases. The experimental data for Feed I, Feed II and Feed III are given in Tables VII, VIII and IX, respectively.

Table VII: The concentrations of ETA in the feed, product and reject (ppm) at different time intervals for Feed-I.

	Initial (t~0)	t~2 hrs.	t~4 hrs.	Final (t~6 hrs.)
RUN-1				
Feed	5.2	4.1	3.7	3.5
Product	-	22.2	30.6	35.5
Reject	-	1.2	0.9	0.7
RUN-2				
Feed	5.4	3.9	3.6	3.1
Product	-	68.7	81.2	96.4
Reject	-	1.7	1.5	1.1
RUN-3				
Feed	5.1	4.3	4.2	3.9
Product	-	27.5	36.2	40.4
Reject	-	0.9	0.6	0.3

Table VIII: The concentrations of Dimethylamine in the feed, product and reject (ppm) at different time intervals for Feed-II.

	Initial (t~0)	t~2 hrs.	t~4 hrs.	Final (t~6 hrs.)
RUN-1				
Feed	4.8	2.9	2.7	2.5
Product	-	35.2	41.5	48.6
Reject	-	1.6	1.2	1.0
RUN-2				
Feed	5.4	3.7	3.1	2.8
Product	-	42.3	48.7	59.0
Reject	-	1.9	1.4	1.2
RUN-3				
Feed	5.2	3.5	3.2	2.7
Product	-	43.7	51.2	55.4
Reject	-	1.6	1.3	0.9



Table IX: The concentrations of ETA and Sodium in the feed, product and reject (ppm)  
at different time intervals for Feed-III.

	Initial (t~0)		t~3 hrs.		Final (t~6 hrs.)	
RUN-1	ETA	Na	ETA	Na	ETA	Na
Feed	5.8	45.3	5.4	40.5	5.1	35.8
Product	-	-	~0	81.1	~0	140.4
Reject	-	-	5.5	36.8	4.8	32.0
RUN-2						
Feed	5.5	44.0	5.3	38.5	4.8	32.0
Product	-	-	~0	92.4	0.52	148.2
Reject	-	-	4.4	37.7	4.3	26.3

## Results

The feed, reject and product samples were collected at the same time at different time intervals. Earlier, the samples were subjected to analysis with Gas Chromatograph using different absorption columns. But the product components could not be clearly identified, and therefore, the product concentrations could not be determined. Several pH analysis and volumetric titrations have also been tried before the product analysis could be successfully done using an Ion Chromatograph.

From the results obtained using IC, quantitative analysis for the components involved was done. Simple material balances is not applicable to these experimental cases because the reject stream is recycled to the feed tank. The feed concentration continuously changes with time as pervaporation takes place. So the rate of change of feed concentration is equal to the rate of change of permeate concentration plus the rate of change of reject concentration. The experiments were repeated when this criterion could not be met. The above criterion was used to experimental data shown in the Tables VII and VIII between the indicated time intervals to study the amine separation, and was satisfactorily obeyed for most of the cases except for the second run in Table VII. The data obtained for the second run in Table VII could be because of some experimental error, hence, cannot be considered. The data for Feed-III shown in Table IX is rather more complex to analyze due to its nature, and the application of above criterion does not result in a definite quantitative explanation. However, due to some consistency in the two runs for the Feed-III, some meaningful conclusions can be certainly drawn qualitatively.

From the product analysis for Feed I and Feed II, the concentrations of Ethanolamine and Dimethylamine were found to be high in the permeate (low rejection) compared to that in reject stream. This indicates the possibility of separation of amines using pervaporation. However, for Feed III, the reverse trend was observed. The permeate mainly consisted of NaCl and only trace amounts of ETA. Therefore, ETA was highly rejected by Nafion membrane in the presence of NaCl. So, the separation of amines is possible in any case, but the distribution of amines into permeate or reject stream is dependent on whether or not any third species is present in the initial feed solution.

The membrane selectivity of ion species  $i$  with respect to species  $j$  is determined by the ratio of the partition coefficients given by (Aptel and Neel, 1986):

$$S_j^i = K_i / K_j \quad (6-1)$$

where, partition coefficient of an ion species,  $K_i$ , is defined as the concentration ratio of ions inside and outside the membrane. The Nafion membrane being of  $K^+$  form, has higher partition coefficient of  $Na^+$  and  $Cl^-$  than ETA, and therefore exhibits more permselectivity for NaCl. Consequently, the rejection of ETA is high in the presence of NaCl.

The experimental results prove conclusively that pervaporation technique can be used for separation of amines. Selectivity of the membrane for a particular species depends not only on the chemical nature of the membrane, but also on the presence of any third component and its type.

## **CHAPTER VII**

### **CONCLUSIONS AND RECOMMENDATIONS**

#### **Conclusions**

- Reverse Osmosis has achieved a tremendous growth in its applications and importance over the past few decades. Its wide acceptance is reflected by increasing number of publications in the field. Future work in this area can lead to further growth of reverse osmosis in all its practical applications, and contribute significantly to the economic prosperity.
- Some major developments have taken place in the preparation of synthetic membranes over the past few years. There is still an immense need for the development of membranes with excellent chlorine resistance and good anti-fouling characteristics.
- Unlike for single solute systems, there are only a few models to describe reverse osmosis with multicomponent system. Modeling of multicomponent systems is of both fundamental and practical interest.
- An analytical technique for predicting membrane performance in reverse osmosis for mixed solute aqueous feed solution systems involving four monovalent ions has been presented. The effect of module geometry can also be investigated. The agreement between predicted and experimental results support the validity of Kimura-Sourirajan

analysis, the basis for the model, and confirm the practical utility of the prediction technique.

- The quality of permeate from reverse osmosis can be enhanced with increase in feed flow rate, operating pressure, mass transfer coefficient on the feed side of the membrane and decrease in feed concentration.
- The values of solute transport parameters is of great importance in determining the ion selectivity of a membrane. This fact can be made use of in establishing theoretical equations for reverse osmosis process design for desalination and other applications.
- Similar trends can be observed in the performance of flat-membrane RO units and spiral-wound modules when subjected to identical changes in the operating variables. The differences in the ion-separation and product flux between the two types of RO units is because of the differences in their inherent designs and mass transfer characteristics.

### **Recommendations**

- Since there is a tremendous need for a lot of research in multicomponent system modeling of reverse osmosis, more attention should be paid in the development of better models in this area.

- There is a lack of osmotic pressure data for various solute systems, which imposes serious restrictions on the universal applicability of any model that is developed. So, there is need for a lot experimental effort to generate of such data.
- The model for the prediction of performance of reverse osmosis membrane for a four component system has been discussed here, and a foundation for further progress has been laid. Based upon this ground work, the prediction technique can be further extended to more number of species.

## BIBLIOGRAPHY

- Allegrezza, A.E., Jr. (1988). Commercial reverse Osmosis Membranes and Modules. In B.S. Parekh (Ed.), Reverse Osmosis Technology: Applications for High-Purity-Water Production, New York, Marcel Dekker, pp. 53-120.
- Aptel, P., Challard, J.C. & Neel, J. (1976). Application of the Pervaporation Process to Separate Azeotropic Mixtures, Journal of Membrane Science, 1, 271.
- Awadalla, F.T., Striez, C. & Lamb, K. (1994). Removal of Ammonium and Nitrate Ions from Mine Effluents by Membrane Technology, Separation Science and Technology, 29(4), pp. 483-495.
- Awadalla, F.T. & Kumar, A. (1994). Opportunities for Membrane Technologies in the Treatment of Mining and Mineral Process Streams and Effluents, Separation Science and Technology, 29(10), pp. 1231-1249.
- Belfort, G. (1984). Synthetic Membrane Processes: Fundamentals and Water Applications. Florida: Academic Press.
- Binning, R.C., Lee, R.C. & Martin, E.C. (1961). Separation of Liquid Mixtures by Permeation, Ind. Eng. Chem., 53, 45.
- Bird, R.B., Stewart, W.E. & Lightfoot, E.N. (1960), Transport Phenomena, New York: John Wiley.
- Burden, R.L., Faires, J.D. (1990). Numerical Analysis, 3<sup>rd</sup> Ed., PWS Publishers.

- Cadotte, J.E. & Petersen R.J. (1990). Thin Film Composite Reverse Osmosis Membranes in M.E., Porter (Ed), Industrial Membrane Technology, Noyes Publications, Park Ridge, NJ, p. 307.
- Cadotte, J.E. (March 1981). U.S. Patent 4,259,183.
- Cadotte, J.E., Petersen, R.J., Larsen, R.E. and Erickson, E.E. (1980). A New Thin Film Composite Reverse Osmosis Membrane, Desalination, 32.
- Cartwright, P.E. (Sept 1995). Useful Applications of Membrane Technologies in Precision Cleaning Processes, Ultrapure Water.
- Castellan, G.W. (1971). Physical Chemistry (2nd Edition). London: Addison Wesley, pp. 297-301.
- Comb, L.F. (July 1994). Going forward with Reverse Osmosis, Chemical Engineering, pp. 90-92.
- Crawford, P.M. (Aug 1992). Membrane Technology becoming an Accepted Alternative, Water and Pollution Control, pp. 10-12.
- Crespo, J.G. & Boddekar, K.W. (1990) Membrane Processes in Separation and Purification, KA Publishers.
- Ericsson, B. & Hallmans, B. (1994). Membrane Applications in raw Water Treatment With and Without Reverse Osmosis Desalination, Desalination, 98, pp. 3-16.
- Finan, M. A. (Apr 1995). Selection of a Novel Multifoulant, Ultrapure Water, pp. 61-65.
- Fleming, H.L. & Slater, C.S. (1990). Theory of Pervaporation, Membrane Handbook, Noyes Ridge Publishers.
- Gurumorthy, K. & Swaminathan T. (1994). Use of Reverse Osmosis in a Chlor Alkali Plant, Desalination, 98, pp. 303-307.



- Harfst, W.F. (Oct 1995). Back to Basics, Ultrapure Water.
- Hoffer, E. & Kedem, O. (1972). Industrial Engineering and Chemical Process Design Development, 11, pp. 221.
- Ikeda, K. & Toaschke, J. (1994). Noble Reverse Osmosis Composite Membrane, Desalination, 96, pp. 113-118.
- Ikeda, T., Muragishi, H., Bairinji, R. & Uemura T. (1994). Advanced Reverse Osmosis Membranes Modules for Novel Ultrapure Water Production Process, Desalination, 98, pp. 391-400.
- Jacobson, J. (1995). Researches investigate the Development of Tolerant Membranes, Water and Irrigation Review, Vol 15, No. 4.
- Kamal, N. (1995). Modeling and Experiments of Aqueous Alcohol Separation via Pervaporation( Ph.D dissertation).
- Kar, S. (1994). Mathematical Modeling of Reverse Osmosis for Ultrapure Water Production(thesis).
- Kar, S., Foutch, G.L. & High M.S. (1995). A Monograph on Reverse Osmosis in High Purity Water Treatment.
- Kedem, O. & Katchalsky, A. (1958). Thermodynamic Analysis of the Permeability of Biological Membranes to Non-Electrolytes, Biochimica et Biophysica Acta, 27, pp. 229-246.
- Ko, A. & Guy D.B. (1988). Brackish and Seawater Desalination, In B.S. Parekh, Reverse Osmosis Technology: Applications for High-Purity Water Production, New York: Marcel Dekker, pp. 236-248.

- Kremen, S.S. & Reidinger, A.B. (1971). Reverse Osmosis Membrane Module( Spiral-Wound Concept), U.S. Dept. of the Interior, Office of Saline Water, Research and Development PR-676.
- Krygier, V. (March 1994). Advanced Ultrafiltration Technology For High-Purity Water, Ultrapure Water, pp. 56-59.
- Lang, K., Chowdhury, G., Matsuura, T. & Sourirajan S. (1994) Reverse Osmosis Performance of Modified Polyvinyl Alcohol Thin-Film Composite Membranes, Journal of Colloid and Interface Science, 166, pp. 239-244.
- Lonsdale, H. K. (1965) Desalination by Reverse Osmosis, Cambridge, MA: MIT press.
- Matsuura, T., Bednas, M.E. & Sourirajan, S. (1974). Reverse Osmosis Separation of single and mixed alcohols in aqueous solutions using porous Cellulose Acetate Membranes, Journal of Applied Polymer Science, 75, pp. 205-211.
- Matsuura, T., Pageau, L. & Sourirajan, S. (1975). Reverse Osmosis Separation of Inorganic solutes in Aqueous solutions using porous Cellulose Acetate Membranes, Journal of Applied Polymer Science, 19, pp. 179-198.
- Noshita, M. (1994). Reverse Osmosis Seawater Desalination for Power Plant, Desalination, 96, pp. 359-368.
- Parsons, R. (1959). Handbook of Electrochemical Constants, Table 73, Butterworths.
- Personal Communication with Dr. Martin S. High & Dr. Gary L. Foutch (May 1996).
- Petersen, R.J. (1993). Composite Reverse Osmosis and Nanofiltration Membranes, Journal of Membrane Science, 83, pp. 81-150.
- Rangarajan, R., Baxter, A.G., Matsuura, T. & Sourirajan, S. (1984). Predictability of Membrane Performance for Mixed Solute Reverse Osmosis Systems. 3. System:

Cellulose Acetate Membrane-Three 1:1 Electrolytes-Water, I & EC Process Design and Development, 23, pp. 367-374.

Rangarajan, R., Majid, M.A., Matsuura, T. & Sourirajan, S. (1985). Predictability of Membrane Performance for Mixed-Solute Reverse Osmosis Systems. 4. System: Cellulose Acetate- Nine Seawater Ions-Water, I & EC Process Design and Development, 24, pp. 977-985.

Rangarajan, R., Matsuura, T., Goodhue, E.C. & Sourirajan, S. (1976). Free Energy Parameters for reverse Osmosis Separations of some Inorganic ions and ion pairs in Aqueous solutions, I & EC Process Design and Development, 15, pp. 529-534.

Rangarajan, R., Matsuura, T., Goodhue, E.C. & Sourirajan, S. (1978a). Free Energy Parameters for Reverse Osmosis Separations of some Inorganic ions and ion pairs in Aqueous solutions, I & EC Process Design and Development, 17, pp. 71-76.

Rangarajan, R., Matsuura, T., Goodhue, E.C. & Sourirajan, S. (1978b). Predictability of Reverse Osmosis Performance of porous Cellulose Acetate Membranes for Mixed uni-univalent Electrolytes in Aqueous solutions, I & EC Process Design and Development, 17, pp. 46-56.

Rangarajan, R., Matsuura, T., Goodhue, E.C. & Sourirajan, S. (1979). Predictability of Membrane Performance for Mixed Solute Reverse Osmosis Systems. 2. System: Cellulose Acetate Membrane- 1:1 and 2:1 Electrolyte-Water, I & EC Process Design and Development, 18, pp. 278-287.

Rautenbach, R. & Albrecht, R. (1989). Membrane Processes, New york: Wiley.

Rautenbach, R. & Mellis, R. (1995). Hybrid Processes Involving Membranes for the Treatment of Highly Organic/Inorganic Contaminated Waste Water, Desalination, 101, pp. 105-113.

Riggs, J.B. (1994). An Introduction to Numerical Methods for Chemical Engineers, 2<sup>nd</sup> Ed., pp. 76-100.

Sourirajan, S. (1970). Reverse Osmosis, New York: Academic Press.

Sourirajan, S. (1977). Reverse Osmosis and Synthetic Membranes: Theory - Technology - Engineering, Ottawa, Canada: National Research Council of Canada Publications.

Sundet, S.A., Arthur S.D., Campos, D., Eckman, T.J. and Brown, R.G. (1987). Aromatic and Cycloaliphatic Polyamide Membrane, Desalination, 64.

Winograd, Y., Solan, A. & Toren, M. (1973). Mass Transfer in Narrow Channels in the Presence of Turbulent Promoters, Desalination, 13, pp. 171-186.

## APPENDIX A

### DERIVATION OF CONCENTRATION POLARIZATION EFFECT IN REVERSE OSMOSIS USING FILM THEORY

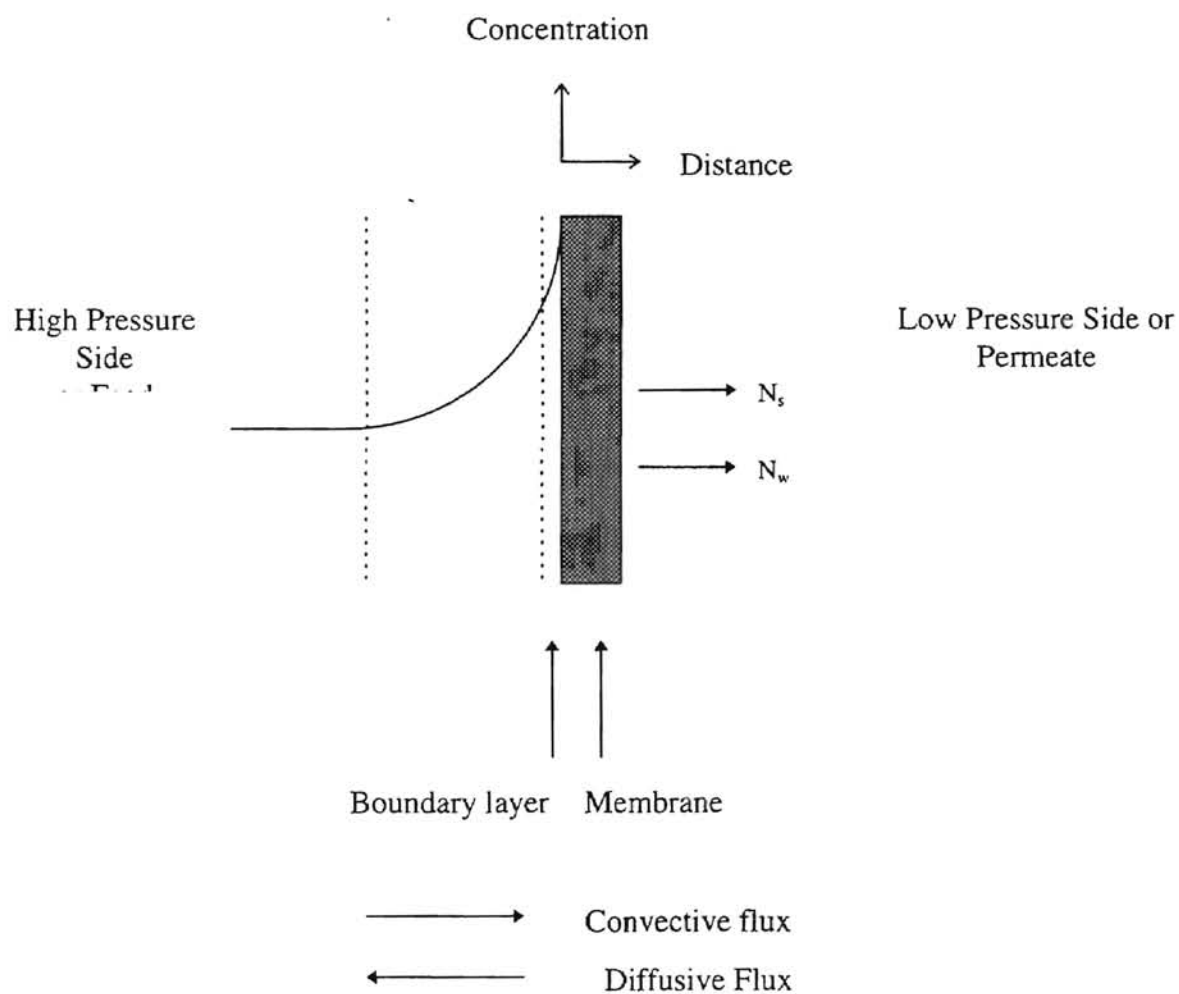


Figure 8: Concentration Polarization Effect

As explained in Chapter II, concentration polarization phenomenon can be derived in two ways. The derivation is based on the film concept of mass transfer across a boundary layer (Bird, 1960). Sourirajan(1970) first proposed the use of film concept to derive the concentration polarization effect in reverse osmosis. The following derivation is based upon the derivation of Sourirajan(1970) and Rautenbach and Albrecht(1989).

Since the net solute flux is the sum of the convective flux and the diffusive flux, which are in opposite direction. The solute flux can be written as,

$$N_S = \text{Convective flux} + (- \text{diffusive flux})$$

or

$$N_S = X_S(N_S + N_W) - cD_{sw} \frac{dX_S}{dy} \quad (\text{A-1})$$

Equation (A-1) can be written in a differential equation form as,

$$\frac{dX_S}{dy} = X_S \frac{(N_S + N_W)}{D_{sw}c} - \frac{N_S}{D_{sw}c} \quad (\text{A-2})$$

Solute flux can be written as ,

$$N_S = X_{S3}(N_S + N_W) \quad (\text{A-3})$$

Substituting Equation (A-3) into Equation (A-2), we have:

$$\frac{dX_S}{dy} = X_S \frac{(N_S + N_W)}{D_{sw}c} - \frac{(N_S + N_W)}{D_{sw}c} X_{S3} \quad (\text{A-4})$$

Referring to the Figure 8, the boundary conditions for the above differential equations are:

$$\text{At } y = 0, X_S = X_{S1} \quad (\text{A-5})$$

$$\text{At } y = L, X_S = X_{S2} \quad (\text{A-6})$$

Solving the differential Equation ( A-4) with the above boundary conditions, we have:

$$X_{S2} = X_{S3} + (X_{S1} - X_{S3}) \exp \left[ \frac{(N_S + N_W)}{c} \frac{L}{D_{SW}} \right] \quad (A-7)$$

Defining the mass transfer coefficient by the film theory (Bird et al.,1960),

$$k = D_{SW} / L \quad (A-8)$$

Substituting the Equation (A-8) into Equation (A-7),

$$X_{S2} = X_{S3} + (X_{S1} - X_{S3}) \exp \left[ \frac{(N_S + N_W)}{kc} \right] \quad (A-9)$$

Using the assumption that  $N_W \gg N_S$ ,  $(N_S + N_W)$  can be effectively replaced by  $N_W$  without significant error. Thus,

$$X_{S2} = X_{S3} + (X_{S1} - X_{S3}) \exp \left[ \frac{N_W}{kc} \right] \quad (A-10)$$

Equation (A-10) gives the concentration of solute in the boundary layer and represents the effect of concentration polarization.

## APPENDIX B

### CORRELATIONS USED IN REVERSE OSMOSIS MODELING

Following are the correlations used in the reverse osmosis model. The Kimura-Sourirajan model is considered here.

- (i) At any given temperature, pressure and feed flow rate, mass transfer coefficient for a solute or ion in terms of NaCl is given by:

$$k_i = k_{\text{NaCl}} [(D_{iW}) / (D_{iW})]^{2/3} \quad (\text{B-1})$$

The above correlation is used for flat membrane RO unit.

- (ii) For spiral-wound modules, the expression for mass transfer coefficient is based upon mesh step model originally proposed by Winograd et al.(1973). It takes into account the effect of promoter nets to increase the turbulence in the feed flow. Using this model, the mass transfer coefficient is related to the diffusivity of the ion, kinematic viscosity of the solution, Area of feed channel and feed flow rate by the following relationship:

$$k = \sigma D_{\text{sw}}^{2/3} \eta^{-1/6} A_{\text{ch}}^{-1/2} \{Q_1\}^{1/2} \quad (\text{B-2})$$

- (iii) Based upon the concept of free-energy parameters, the following relationships were developed by Matsuura et al. (1975) and Rangarajan et al. (1976).



$$\ln\left(\frac{D_{iM}K}{\delta}\right) = \ln C_{NaCl} + \sum \left(-\frac{\Delta\Delta G}{RT}\right)_i \quad (B-3)$$

where,

$$\ln C_{NaCl} = \ln\left(\frac{D_{iM}K}{\delta}\right)_{NaCl} - \left[ \left(-\frac{\Delta\Delta G}{RT}\right)_{Na^+} + \left(-\frac{\Delta\Delta G}{RT}\right)_{Cl^-} \right] \quad (B-4)$$

## APPENDIX C

```

C*****
C
C          PROGRAM SISOMSO
C*****
C
C  PROGRAM TO PREDICT THE PERFORMANCE OF MULTICOMPONENT
C  REVERSE OSMOSIS SYSTEM INVOLVING FOUR MONOVALENT IONS,
C  NAMELY, SODIUM, POTASSIUM, CHLORIDE AND NITRATE.
C
C  THIS PROGRAM IS BASED ON KIMURA-SOURIRAJAN MASS
C  TRANSPORT MODEL (KSA MODEL).
C
C  THIS PROGRAM CAN BE USED FOR BOTH FLAT-MEMBRANE REVERSE
C  OSMOSIS UNIT AND SPIRAL-WOUND MODULE.
C
C  PREPARED BY KALYAN S. WUNNAVA & DR. GARY L. FOUTCH
C          DEPARTMENT OF CHEMICAL ENGINEERING
C          OKLAHOMA STATE UNIVERSITY
C          STILLWATER, OKLAHOMA-74075
C*****
C*****NOMENCLATURE*****
C
C  IN THIS SECTION, ALL THE VARIABLES USED IN THE MODEL ARE
C  IDENTIFIED. THEY ARE AS FOLLOWS:
C
C  A          =  MEMBRANE PERMEABILITY CONSTANT
C  ACH        =  AREA OF THE FEED CHANNEL IN SPIRAL MODULE
C  AM         =
C  AL         =  ALPHA DEFINED BY EQUATION (3-11)
C  BAV        =  B-AVERAGE DEFINED BY EQUATION (3-17)
C  BE         =  BETA DEFINED BY EQUATION (3-38)
C  C          =  MOLAR DENSITY OF THE SOLUTION ASSUMED TO
C               BE CONSTANT IN ALL THE PHASES
C  CH         =  CONCENTRATION OF HYDROGEN IONS
C  DELTA      =  SMALL INCREMENT IN THE MOLE FRACTION OF
C               AN IONIC SPECIES
C  DET        =  DETERMINANT OF JACOBIAN MATRIX
C  D2         =  X(12) DEFINED BY EQUATION (3-29)
C  D3         =  X(22) DEFINED BY EQUATION (3-30)
C  D4         =  X(32) DEFINED BY EQUATION (3-31)
C  D5         =  X(42) DEFINED BY EQUATION (3-32)
C  DNA        =  DIFFUSIVITY OF SODIUM ION

```

C	DK	=	DIFFUSIVITY OF POTASSIUM ION
C	DCL	=	DIFFUSIVITY OF CHLORIDE ION
C	DNO3	=	DIFFUSIVITY OF NITRATE ION
C	ETA	=	KINEMATIC VISCOSITY OF THE SOLUTION (CP)
C	EF2	=	NUMERATOR OF OMEGA1 DEFINED BY EQUATION (3-45)
C	FF2	=	DENOMINATOR OF OMEGA1 DEFINED BY EQUATION (3-45)
C	ES2	=	NUMERATOR OR SECOND TERM OF EQUATION (3-43)
C	ES2	=	DENOMINATOR OF SECOND TERM OF EQUATION (3-43)
C	EF3	=	NUMERATOR OF OMEGA2 DEFINED BY EQUATION (3-48)
C	FF3	=	DENOMINATOR OF OMEGA2 DEFINED BY EQUATION (3-48)
C	ES3	=	NUMERATOR OR SECOND TERM OF EQUATION (3-46)
C	ES3	=	DENOMINATOR OF SECOND TERM OF EQUATION (3-46)
C	EF2	=	NUMERATOR OF OMEGA3 DEFINED BY EQUATION (3-46)
C	FF2	=	DENOMINATOR OF OMEGA3 DEFINED BY EQUATION (3-51)
C	ES2	=	NUMERATOR OR SECOND TERM OF EQUATION (3-49)
C	ES2	=	DENOMINATOR OF SECOND TERM OF EQUATION (3-49)
C	FUNJAC	=	SUBROUTINE NAME TO CALCULATE FINITE JACOBIAN
C	FUNCTN	=	SUBROUTINE TO CALCULATE THE FUNTION VALUES
C	FSAVE	=	ARBITRARY VARIABLE TO STORE VALUE OF A FUNCTION
C	FTOL	=	FUNCTION TOLERANCE
C	I	=	ARBITRARY VARIABLE
C	IT	=	ITERATION NUMBER
C	IVBL	=	ARBITRARY VARIABLE
C	ITEST	=	ARBITRARY VARIABLE
C	IPVTMT	=	PIVOT ELEMENT
C	IROW	=	ARBITRARY VARIABLE
C	J	=	ARBITRARY VARIABLE
C	JCOL	=	ARBITRARY VARIABLE
C	KCOL	=	ARBITRARY VARIABLE

C	LUDCMP	=	SUBROUTINE NAME TO SOLVE THE TRI- DIAGONA MATRIX BY L-U DECOMPOSITION
C	M	=	ARBITRARY VARIABLE
C	MAXIT	=	MAXIMUM NUMBER OF ITERATIONS
C	N	=	NUMBER OF ARRAY LOCATIONS FOR NUMBER OF IONS, SHOULD BE GREATER THAN OR EQUAL 4
C	NDIM	=	ARBITRARY VARIABLE
C	NLESS	=	ARBITRARY VARIABLE
C	NEWTON	=	SUBROUTINE TO SOLVE THE NON-LINEAR EQUATIONS BY NEWTON'S METHOD
C	PH	=	PH OF THE PERMEATE
C	PRE	=	OPERATING PRESSURE
C	Q1	=	FEED FLOW
C	Q2	=	REJECT FLOW
C	Q3	=	PERMEATE FLOW
C	RNA	=	FLUX OF SODIUM ION
C	RK	=	FLUX OF POTASSIUM ION
C	RCL	=	FLUX OF CHLORIDE ION
C	RNO3	=	FLUX OF NITRATE ION
C	RG	=	GAMMA DEFINED BY EQUATION (3-38)
C	RKAV	=	AVERAGE VALUE OF MASS TRANSFER COEFFICIENT DEFINED BY EQUATION ( 3-55)
C	RKW	=	DISSOCIATION CONSTANT OF WATER
C	SA	=	ARBITRARY VARIABLE
C	SIGMA	=	QUANTITY DEFINED BY EQUATION (3-54)
C	SUM	=	ARBITRARY VARIABLE
C	SOLVER	=	SUBROUTINE FOR MATRIX MANIPULATIONS
C	T1	=	QUANTITY DEFINED BY EQUATION (3-44)
C	T2	=	QUANTITY DEFINED BY EQUATION (3-47)
C	T3	=	QUANTITY DEFINED BY EQUATION (3-50)
C	TMPVT	=	ARBITRARY VARIABLE
C	X	=	MOLE FRACTION OD IONIC SPECIES
C	X(1)	=	PRODUCT FLUX
C	X(2)	=	MOLE FRACTION OF SODIUM ION
C	X(3)	=	MOLE FRACTION OF POTASSIUM ION
C	X(4)	=	MOLE FRACTION OF CHLORIDE ION
C	X(5)	=	MOLE FRACTION OF NITRATE ION
C	RNA	=	REJECTION OF SODIUM ION
C	RK	=	REJECTION OF POTASSIUM ION
C	RNO3	=	REJECTION OF NITRATE ION
C	RCL	=	REJECTION OF CHLORIDE ION
C	XY	=	RECOVERY
C	XTOL	=	TOLERANCE FOR IONIC MOLR FRACTION
C	Y	=	RECOVERY
C			

```

C*****
C*****READING THE DATA *****
C
  OPEN ( UNIT =9 FILE = 'DATA', STATUS ='OLD')
  REWIND 9
  OPEN (UNIT =10FILE = 'OUTPUT', STATUS= 'NEW')
  REWIND 10
  REAL X(5), F(5), DELTA, XTOL, FTOL, KNA, KK, KCL, KNO3
  REAL KAV
  INTEGER N,MAXIT
  EXTERNAL FUNCTN,FUNJAC
  DATA DELTA, XTOL, FTOL, M/ 0.125E-04, 1.0E-08, 1.0E-08, 0/
  DATA MAXIT, N/150, 5/
  COMMON/CONSTANTS/XF2,XF3, PRE, A, T1,T2,T3

C
C  READ THE CONSTANTS FROM THE INPUT DATA FILE, 'DATA'
C  FIRST CHOOSE THE OPTION OF PREDICTION FOR FLAT MEMBRANE
C  RO UNIT OR SPIRAL WOUND MODULE. FOR  FLAT RO UNIT, ENTER
C  CHOICE=1 AND FOR SPIRAL MODULE ENTER ANY NUMBER
C
C  READ THE VALUES FROM THE DATA FILE IN THE FOLLOWING
  ORDER: CHOICE, XF2,XF3,PRE, A, T1, T2, T3, Q1, AM, X(1), SIGMA, ACH
  READ (9,*) CHOICE
  IF (CHOICE.EQ.1.0) THEN
    READ(9,*) XF2, XF3, PRE, A, KNACL, T1, T2, T3, Q1, AM, X(1), RKW
  ELSE
    READ(9,*) XF2, XF3, PRE, A, KNACL, T1, T2, T3, Q1, AM, X(1), SIGMA,
    ACH, RKW
  ENDIF
  CLOSE(9)

C *****
C                               MAIN PROGRAM
C *****
C  GUESS VALUES FOR MOLE FRACTIONS TO BE 10 % OF THEIR FEED
C  VALUES
  X(2)=XF2/10.0
  X(3)=XF3/10.0
  X(4)=XF2/10.0
  X(5)=XF3/10.0

C
C  UNIVERSAL CONSTANTS IN THE PROGRAM
  ETA  = 0.9
  DNA  = 1.35 E-05
  DCL  = 2.03 E-05
  DNO3 = 1.61 E-05

```

```

DK    = 1.98 E-05
DNACL = 1.65E-05
C
C    SELECTING FLAT RO UNIT OR SPIRAL WOUND
C
    IF (CHOICE.EQ.1.0) THEN
        KNA = KNACL*(DNA/DNACL)**0.667)
        KK  = KNACL*(DK/DNACL)**0.667)
        KCL = KNACL*(DCL/DNACL)**0.667)
        KNO3 = KNACL*(DNO3/DNACL)**0.667)
        KAV = (KNA+KK+KCL+KNO3)/4.0
    ELSE
        FACTOR=SIGMA*(ETA**(-0.66&))*(ACH(-0.5)*SQRT(Q1/60)
        KNA = FACTOR*(DNA**0.667)
        KK  = FACTOR*(DK**0.667)
        KCL = FACTOR*(DCL**0.667)
        KNO3 = FACTOR*(DNO3**0.667)
        KAV =((KNA+KK+KCL+KNO3)/4.0
    ENDIF
C
C    CALLING SUBROUTINE NEWTON
C
    CALL NEWTON(FUNCTN, N, MAXIT, X, F, DELTA, XTOL, FTOL, M, KAV)
    Q3= 60*18.0*AM*X(1)
    Q2=Q1-Q3
    Y=(Q3/Q1)*100.0
    RNA = ((XF2-X(2))/XF2)*100.0
    RK  = ((XF3-X(3))/XF3)*100.0
    RCL = ((XF2-X(4))/XF2)*100.0
    RNO3 = ((XF3-X(5))/XF3)*100.0
C
101  FORMAT (///'THE MOLE FRACTIONS OF IONS IN PERMEATE ARE:'/)
111  FORMAT (///'THE IONIC FLUXES, IN GMOLE PERSQ CM ARE:'/)
121  FORMAT (///'THE PRODUCT FLUX IN GMOLE PER SEC SQ CM IS:'/)
131  FORMAT (///'PERMEATE FLOW, Q3, IN CU.CM/SEC IS:'/)
141  FORMAT (///'REJECT FLOW Q2, IN CU. CM/SEC IS:'/)
151  FORMAT (///'THE RECOVERY OF THE SYSTEM IS:'/)
161  FORMAT (///REJECTION OF IONS IS:'/)
171  FORMAT (///PH OF THE PERMEATE IS:'/)
201  FORMAT (/T6, F10.8/)
211  FORMAT (/T6, D15.6/)
221  FORMAT (/T6, F7.2/)
C
C    PRINTING MOLE FRACTIONS

```

```

WRITE(*, 101)
WRITE(10, 101)
WRITE(*, 201) (X(I), 2, N)
WRITE(10, 201) (X(I), 2, N)
C
C PRINTING IONIC FLUXES
C
WRITE(*, 111)
WRITE(10, 111)
WRITE (*, 211) X(2)*X(1)
WRITE (*, 211) X(3)*X(1)
WRITE (*, 211) X(4)*X(1)
WRITE (*, 211) X(5)*X(1)
WRITE (10, 211) X(2)*X(1)
WRITE (10, 211) X(3)*X(1)
WRITE (10, 211) X(4)*X(1)
WRITE (10, 211) X(5)*X(1)
C
C PRINTING WATER FLUX
C
WRITE (*,121)
WRITE (10,121)
WRITE (*,221) X(1)
WRITE (10,221) X(1)
C
C PRINTING PERMEATE FLOW
C
WRITE (*,131)
WRITE (10,131)
WRITE (*,221) Q3
WRITE (10,221) Q3
C
C PRINTING REJECT FLOW
C
WRITE (*,141)
WRITE (10,141)
WRITE (*,221) Q2
WRITE (10,221) Q2
C
C PRINTING RECOVERY
C
WRITE (*,151)
WRITE (10,151)
WRITE (*,221) Y
WRITE (10,221) Y

```

```

C
C PRINTING IONIC REJECTION
C
WRITE(*, 161)
WRITE(10, 161)
WRITE(*, 221) RNA, RK, RCL, RNO3
WRITE(10, 221) RNA, RK, RCL, RNO3
C
C PRINTING THE PH OF THE PERMEATE
C
WRITE (*,171)
WRITE (10,171)
WRITE (*,221) PH
WRITE (10,221) PH
C
P1=X(2)+X(3)
P2=X(4)+X(5)
B=P2-P1
BM=B*55.55(1-B)
CH=BM+SQRT(BM**2.0 + 4.0*RKW)/2.0
PH= -LOG(CH)
STOP
END
C END OF THE MAIN PROGRAM

CALL NEWTON(FUNCTN,N,MAXIT,X,F,DELTA,XTOL,FTOL,M)
WRITE (*,100)
100 FORMAT(///"THE VALUES OF X ARE:'/)
WRITE(*,200)(X(I),I=1,N)
200 FORMAT (/T6,F10.8/)
GOTO 2500
WRITE (*,160)
FORMAT(///"THE VALUES OF X ARE:'/)
WRITE(*,170)(X(I),I=1,N)
FORMAT (/T6,F10.8/)
C
STOP
END
C
C*****
C SUBROUTINE LUDCMP
C*****
C THIS SUBROUTINE CALCULATES THE TRIDIAGONAL MATRIX USING
C L-U DECOMPOSITION
C

```



```

C      DO 50 JROW=IPLUS1,N
      IF (A(JROW,I).NE.0.0) THEN
      A(JROW,I)=A(JROW,I)/A(I,I)
      DO 60 KCOL=IPLUS1,N
      A(JROW,KCOL)=A(JROW,KCOL)-A(JROW,I)*A(I,KCOL)
60    CONTINUE
      ENDIF
50    CONTINUE
20    CONTINUE
C
C      IF(ABS(A(N,N)).LT.1.0E-05) THEN
      WRITE(*,*) 'MATRIX IS SING OR NEAR SING'
      DET=0.0
      RETURN
      ENDIF
C
C      COMPUTE DET. OF MATRIX
      DO 70 I=1,N
      DET=DET*A(I,I)
70    CONTINUE
      RETURN
      END
C
C*****
C      SUBROUTINE SOLVER
C*****
      SUBROUTINE SOLVER(A,N,IPVT,B,NDIM)
C
      REAL A(NDIM,N),B(N),X(10),SUM
      INTEGER IPVT(N),N,NDIM,IROW,JCOL,I
C
      DO 10 I=1,N
      X(I)=B(IPVT(I))
10    CONTINUE
C
C      DO 20 IROW=2,N
      SUM=X(IROW)
      DO 30 JCOL=1,(IROW-1)
      SUM=SUM-A(IROW,JCOL)*X(JCOL)
30    CONTINUE
      X(IROW)=SUM
20    CONTINUE

```

```

C
C
      B(N)=X(N)/A(N,N)
      DO 40 IROW=(N-1),1,-1
      SUM=X(IROW)
      DO 50 JCOL=(IROW+1),N
      SUM=SUM-A(IROW,JCOL)*B(JCOL)
50    CONTINUE
      B(IROW)=SUM/A(IROW,IROW)
40    CONTINUE
      RETURN
      END

C
C*****
C                      SUBROUTINE  NEWTON
C*****
C  THIS SUBROUTINE SOLVES THE SYSTEM OF EQUATIONS USING
C  NEWTON'S METHOD USING THE CONVERGENCE CRITERIA THAT IS
C  SPECIFIED. NEWTON CALLS THE OTHER SUBROUTINES TO
C  PERFORM
C  FUNTION EVALUATIONS, JACOBIAN CALCULATION AND MATRIX
C  MANIPULATIONS. IT REPEATS THIS PROCEDURE FROM THE INITIAL
C  GUESS VALUES TILL THE POINT OF SOLUTION TO THE EQUATIONS.
C
      SUBROUTINE NEWTON(FUNCTN,N,MAXIT,X,F,DELTA,XTOL,FTOL,M)
      REAL X(N),F(N),DELTA,XTOL,FTOL
      INTEGER N,MAXIT,M
      REAL A(10,10),XSAVE(10),FSAVE(10),B(10),DET
      COMMON A,XSAVE,FSAVE
      INTEGER IPVT(10),IT,IVBL,ITEST,IFCN,IROW
      EXTERNAL FUNCTN,FCNJ
C  BEGIN ITERATIONS
      DO 100 IT = 1,MAXIT
      CALL FUNCTN(N,X,F)
C
C  CHECK FOR FUNCTION TOLERANCE
      ITEST=0
      DO 20 IFCN=1,N
      IF(ABS(F(IFCN)).GT.FTOL) ITEST=ITEST+1
20    CONTINUE
      IF (M.EQ.0)THEN
      PRINT 1000,IT,X
      PRINT 1001,F
      ENDIF
C

```

```

        IF (ITEST.EQ.0)THEN
        M =2
        RETURN
        ENDIF
C      CALLING OTHER SUBROUTINES
C
        CALL FUNJAC(FUNCTN,B,N,X,F,DELTA)
        CALL LUDCMP(A,N,IPVT,10,DET)
        CALL SOLVER(A,N,IPVT,B,10)

C      MATRIX TOO ILL-CONDITIONED??
C
        DO 70 IROW = 1,N
        IF(ABS(A(IROW,IROW)).LE.1.0E-6)THEN
        M=-2
        PRINT 1003
        RETURN
        ENDIF
70    CONTINUE
C      CHECK FOR MOLE FRACTION TOLERANCE
C
        ITEST =0
        DO 80 IVBL=1,N
        X(IVBL)=XSAVE(IVBL)+B(IVBL)
        IF (ABS(B(IVBL)).GT.XTOL) ITEST=ITEST+1
80    CONTINUE
C
        IF (ITEST.EQ.0) THEN
        M=1
        IF(M.EQ.0) PRINT 1002,IT,X
        RETURN
        ENDIF

C
100    CONTINUE
        M=-1
        RETURN
1000   FORMAT('AFTER ITER NUM',I3,'X AND F ARE:'//10F13.8)
1001   FORMAT(/10F13.8)
1002   FORMAT('AFTER ITER NUM',I3,'X VALUES ARE:'//10F13.5)
1003   FORMAT('CANNOT SOLVE THE SYS, MAT NER SING')
        END
C*****
C                                SUBROUTINE FUNJAC
C*****

```

C THIS SUBROUTINE EVALUATES THE JACOBIAN OF FUNCTIONAL  
MATRIX USING FINITE DIFFERENCE JACOBIAN. HERE FIRST  
DERIVATIVE OF THE FUNCTIONS IS CALCULATED BY FUNCTION  
DIFFERENGE DIVIDED BY INCREMENTAL CHANGE IN THE VALUE OF X

C  
SUBROUTINE FUNJAC(FUNCTN,B,N,X,F,DELTA)  
INTEGER N  
REAL X(N),F(N),DELTA  
INTEGER IROW,JCOL  
REAL A(10,10),FSAVE(10),XSAVE(10),B(10)  
COMMON A,XSAVE,FSAVE  
DO 10 IROW=1,N  
FSAVE(IROW)=F(IROW)  
XSAVE(IROW)=X(IROW)  
10 CONTINUE

C  
DO 50 JCOL=1,N  
X(JCOL)=XSAVE(JCOL)+DELTA  
CALL FUNCTN(N,X,F)  
DO 40 IROW=1,N  
A(IROW,JCOL)=(F(IROW)-FSAVE(IROW))/DELTA  
40 CONTINUE

C  
X(JCOL)=XSAVE(JCOL)  
50 CONTINUE

C  
DO 60 IROW=1,N  
B(IROW)=-FSAVE(IROW)  
60 CONTINUE  
RETURN  
END

C\*\*\*\*\*

C SUBROUTINE FUNCTN

C\*\*\*\*\*

C THIS SUBROUTINES EVALUATES THE VALUES OF THE FUCNTIONS  
DEFINED BY EQUATIONS (3-22), (3-42), (3-46), (3-49) AND (3-52)

C  
SUBROUTINE FUNCTN (N,X,F,KAV)  
COMMON/CONSTANTS/XF2, XF3,PRE, A, T1,T2  
INTEGER N  
REAL X(N), F(N)

C  
C =5.4E-02  
BAV =1100  
BE =5.1054

```

RG    =0.08835
Z2    =0.04527
Z3    =0.05372
Z4    =0.06818
Z5    =0.06602

```

```
AL=EXP(X(1)/(RKAV*C))
```

C

```

D2=X(2)+(XF2-X(2))*AL
D3=X(3)+(XF3-X(3))*AL
D4=X(4)+(XF4-X(4))*AL
D5=X(5)+(XF5-X(5))*AL

```

```

EF2=(D4+BE*D50
FF2=(D2+D2/RG)

```

```

EF3=EF2
FF3=(D3+D2/RG)

```

```

EF4=FF2
FF4=EF2

```

```

EF5=FF2
FF5=(D5+D4/BE)

```

```

PRINT*, 'AL=', AL
PRINT*, 'EF2=', EF2, 'FF2=', FF2
PRINT*, 'ES2=', ES2, 'FS2=', FS2
PRINT*, 'EF3=', EF3, 'FF3=', FF3
PRINT*, 'ES3=', ES3, 'FS3=', FS3
PRINT*, 'EF4=', EF4, 'FF4=', FF4
PRINT*, 'ES4=', ES4, 'FS4=', FS4
PRINT*, 'EF5=', EF5, 'FF5=', FF5
PRINT*, 'ES5=', ES5, 'FS5=', FS5

```

C

C

C

```
***** FUNCTIONS REPRESENTATION *****
```

```

F(1)=X(1)-A*PRE+A*BAV*(2*XF2+2*XF3-X(2)-X(3)-X(4)-(X5))*AL
F(2)=X(2)-Z2*T1*(D2*SQRT(EF2/FF2)-X(2)*SQRT(ES2/FS2))/X(1)
F(3)=X(3)-Z3*T2*(D3*SQRT(EF3/FF3)-X(3)*SQRT(ES3/FS3))/X(1)
F(4)=X(4)-Z4*T1*(D4*SQRT(EF4/FF4)-X(4)*SQRT(ES4/FS4))/X(1)
F(5)=X(5)-Z5*T3*(D4*SQRT(EF5/FF5)-X(5)*SQRT(ES5/FS5))/X(1)
PRINT*, F
RETURN
END

```

VITA

Kalyan S. Wunnava

Candidate for the Degree of

Master of Science

Thesis: MODELING OF REVERSE OSMOSIS AND PREDICTION OF REVERSE  
OSMOSIS MEMBRANE PERFORMANCE

Major Field: Chemical Engineering

Biographical:

Personal Data: Born in Cuttack, Orissa, India, September 29, 1973, the son of  
Krishna Rao and Valli Lakshmi Wunnava.

Education: Graduated from St. George's Grammar School, Hyderabad, Andhra  
Pradesh, India, in May, 1990; received Bachelor of Technology degree in  
Chemical Engineering at Osmania University, India in June, 1994;  
completed requirements for Master of Science degree in Chemical  
Engineering at Oklahoma State University in May, 1997.

Professional Experience: Employed as a teaching assistant and research assistant,  
School of Chemical Engineering, Oklahoma State University.